TIDAL WAVE HEIGHT ANALYSIS AT THE COAST PAKNAM TACHIN , KO SICHANG AND HUA-HIN

SURATTANA SRIJUKKRAWALWUT

A THESIS SUBMITTED IN PARTIAL FULFILLMENT
OF THE REQUIREMENTS FOR
THE DEGREE OF MASTER OF SCIENCE (APPLIED MATHEMATICS)
FACULTY OF GRADUATE STUDIES
MAHIDOL UNIVERSITY
2000

ISBN 974-664-213-8

Thesis
entitled

TIDAL WAVE HEIGHT ANALYSIS AT THE COAST

PAKNAM TACHIN , KO SICHANG AND HUA-HIN

Surattana Srijukkrawalwut
.....
Miss. Surattana Srijukkrawalwut
Candidate

I Ming Tang
.....
Prof. I Ming Tang, Ph.D
Major-advisor

Montip Tiensuwan
.....
Assoc. Prof. Montip Tiensuwan, Ph.D.
Co-advisor

.....
Prof. Liangchai Limlomwongse,
Ph.D.
Dean
Faculty of Graduate Studies

Montip Tiensuwan
.....
Assoc.Prof. Montip Tiensuwan, Ph.D.
Chairman
Master of Science Programme
in Applied Mathematics
Faculty of Science

Thesis
entitled

TIDAL WAVE HEIGHT ANALYSIS AT THE COAST PAKNAM TACHIN , KO SICHANG AND HUA-HIN

Was submitted to the Faculty of Graduate Studies, Mahidol University
For the degree of Master of Science (Applied Mathematics)

On
May 18, 2000

Miss. Surattana Srijukkrawalwut
Candidate

Prof. I Ming Tang, Ph.D.
Chairman

Assoc.Prof. Montip Tiensuwan, Ph.D.
Member

Assoc.Prof. Pongtip Winotai, Ph.D.
Member

Prof. Liangchai Limlomwongse
Ph.D.
Dean
Faculty of Graduate Studies
Mahidol University

Prof. Amaret Bhumiratana,
Ph.D.
Dean
Faculty of Science
Mahidol University

ACKNOWLEDGEMENT

I would like to express my sincere gratitude and deep appreciation to Prof. I Ming Tang, my Principle Supervisor for his guidance, invaluable advice, supervision and encouragement throughout this research which have enabled me to complete this thesis successfully. I am equally grateful to Assoc.Prof. Montip Tiensuwan my Associate Supervisor and Assoc.Prof. Pongtip Winotai my External Examiner for their constructive comment and advice about this thesis.

I owe an unending gratitude to Harbour Department , Port Authority of Thailand and Hydrographic Department for observation data. In particular I wish to thank Mr. Jirarath Sungnul for his great assistance in programming. I also would like to thank to staff of the Department of Mathematics, Mahidol University for their co-operation and generous assistance.

I am particularly indebted to the National Science and Technology Development Agency (NSTDA) and the Faculty of Science, Mahidol University for granting the Institutional Strengthening Program scholarship which enables me to undertake this study.

Surattana Srijukkrawalwut

3836841 SCAM/M : MAJOR : APPLIED MATHEMATICS ;
M.Sc. (APPLIED MATHEMATICS)
KEYWORDS : TIDAL ANALYSIS / TIDAL WAVE / MIXED TIDE /
DATA ASSIMILATION

SURATTANA SRIJUKKRAWALWUT : TIDAL WAVE HEIGHT ANALYSIS AT THE COAST PAK NAM TACHIN,KO SICHANG AND HUA-HIN. THESIS ADVISORS : I MING TANG, Ph.D. , MONTIP TIENSUWAN, Ph.D.
87 p. ISBN 974-664-213-8

The heights of the tides at a particular location and at a particular time are often needed. Direct observation of the heights of the tides can only be made at some limited number of sites. Therefore to forecasting the heights of the tides at other locations, methods have to be developed to give predicted heights. Two methods will be reviewed, Least Square Best Fit model and the Data Assimilation method.

The latter method is called the Data Assimilation method. This method is based on the use of the equation of fluid motion as constraints as the values of the parameters in a model which will approximate the full set of hydrodynamic equations.

To compare the two methods, we have analyzed the observation data on the tidal height at three stations, Pak Nam Tachin , Ko Sichang and Hua-Hin in 1996. The sum square error method has been used to determine which techniques provides for both prediction.

3836841 SCAM/M : สาขาวิชา : คณิตศาสตร์ประยุกต์ ; วท.ม. (คณิตศาสตร์ประยุกต์)

สุรัตนา ศรีจักรวาลวุฒิ : การวิเคราะห์ระดับน้ำขึ้นน้ำลง ณ ชายฝั่ง ปากน้ำท่าจีน เกาะสีชัง และหัวหิน (TIDAL WAVE HEIGHT ANALYSIS AT THE COAST PAK NAM TACHIN , KO SICHANG AND HUA-HIN). คณะกรรมการควบคุมวิทยานิพนธ์ : I Ming Tang, Ph.D. , มนต์ทิพย์ เทียนสุวรรณ, Ph.D. 87 หน้า ISBN 974-664-213-8

ความถูกต้องของระดับน้ำขึ้นน้ำลงเป็นที่ต้องการและมีความสำคัญในหลายสาขา ข้อมูลของระดับน้ำขึ้นน้ำลงที่ได้จากการสังเกตนั้นถูกจำกัดด้วยจำนวนสถานี ดังนั้นการศึกษาตัวแบบด้วยวิธีต่าง ๆ จึงได้รับการพัฒนาเพื่อใช้ในการทำนายระดับน้ำขึ้นน้ำลง วิธีที่เราจะกล่าวถึงคือ วิธี Least Square Best Fit. และ วิธี Data Assimilation.

วิธี Data Assimilation. เป็นวิธีที่ใช้พื้นฐานของสมการการเคลื่อนที่ของของเหลวมาเป็นเงื่อนไขทางกายภาพในการคำนวณหาค่าพารามิเตอร์ต่าง ๆ ของตัวแบบ

การเปรียบเทียบผลลัพธ์ของวิธีทั้งสอง โดยการวิเคราะห์ข้อมูลที่ได้จากการสังเกตจาก 3 สถานี คือ ปากน้ำท่าจีน เกาะสีชัง และ หัวหิน ในปี 1996 และใช้ Sum Square Error (SSE) เป็นเครื่องมือในการเปรียบเทียบตัวแบบที่ใช้ในการทำนายระดับน้ำขึ้นน้ำลงของทั้งสองวิธี

LIST OF CONTENTS

LIST OF TABLES

LIST OF FIGURES

PAGE

PAGE

PAGE

CHAPTER I

INTRODUCTION

General

Moving water has a special fascination for man. The regular tidal movements of coastal seas must have challenged human imagination from earliest times. The ancients who were able to link the regular movements of the sea to the movements of the sun and moon regarded tides as a tangible terrestrial sign of the power of the celestial gods. For them the tides had religious significance. For us there are obviously many practical and scientific reasons for needing to know about and understand the dynamics of the oceans and coastal seas.

The Equilibrium tidal model developed from Newton's theory of gravitation consists of two symmetrical tidal bulges, directly under and directly opposite the moon or sun. The individual high water bulges would track around the earth, moving from east to west in steady progression. These characteristics are however not those of the observed tides.

Movements of water on the surface of the earth must obey the physical laws represented by the hydrodynamic equations of continuity and momentum balance. We shall see that this means they must propagate as long waves. Any propagation of a wave from east to west around the earth would be impeded by the continental boundaries running from north to south.

Water movements are affected by the rotation of the earth. The tendency for water movement to maintain a uniform direction in absolute space means that it performs a curved path in the rotating frame of reference within which we make observations. Alternatively, motion in a straight line on a rotating earth is curved in absolute space and must be sustained by forces at right angles to the motion. These effects are represented by the Coriolis accelerations in the hydrodynamic equations. The solutions to the equations show that certain modified forms of wave motion are possible.

Accurate information on tides is needed for many geophysical studies, such as those of the Earth's rotation and the evolution of the moon's orbit (1), for modern space geodesy (2), and for new oceanographic observation techniques such as acoustic tomography (3). Improved information is also needed for the study of tides themselves.

Although satellite altimeters have been developed primarily to monitor minute changes in the slope of the ocean surface due to non – tidal circulation (4), they also supply the best data set ever obtained for studying tides globally. Even though it has an unusual sampling rate and more severe error problems, a satellite altimeter operates as a huge number of open-ocean tide gauges.

On 10 August 1992, the United States and France launched their joint TOPEX/POSEIDON (T/P) satellite. This mission is producing observations of the global sea surface elevation with an accuracy of 5 cm. everywhere, with much better accuracy over some parts of the ocean (5). Designed for a lifetime of 3 to 5 years, the mission is providing the data required to describe and to understand the dynamics of ocean circulation. The mission has sampling adequate to analyze the time variability of

the ocean circulation and its climatic consequences. In addition, the system is working as a powerful global tide gauge.

For tidal analysis the T/P mission (5) has provided two major improvements over earlier satellite altimeters. The first improvement results from the satellite's orbital configuration (66° inclination, 1336-km altitude, and 9.916-day repeat period), chosen so that tidal aliases are well removed from expected oceanographic signals. Table 1.1 lists the data aliasing periods for the eight major ocean tide constituents, for Geosat (17-day repeat orbit), European Remote Sensing satellite 1 (ERS1) (35-day repeat orbit), and T/P (10-day repeat orbit). T/P is the best of the three satellites for tidal mapping. The aliased periods are 62 days for tidal component M_2 , 59 days for tidal component S_2, and 50 days for tidal component N_2; with the longest aliased period being 173 days for tidal component K_1. However, several of these alias stet periods are close, so that the separation of the corresponding components theoretical requires quite long series of observations e.g., nearly 3 years to separate tidal components M_2 and S_2. These are not yet available. The second improvement resulting from the T/P mission is that the error budget is lower than for any earlier mission.

After only 1 year of data collection, the data from the T/P mission has already produced improved tidal models. Even the simpler empirical methods of tidal modeling , based on direct Fourier analysis (6) or using admittance (7) have been successfully applied. To overcome the aliasing constraints, which are particularly severe for these direct approaches with only 1 year of measurement, it has been necessary to bin the data on quite large grid boxes of several degrees in order to

sample a wider range of phases. These empirical methods lead to solutions on coarse grids, which can be used as corrections to existing tidal models.

Table 1.1 Tidal aliasing periods of the eight major ocean tide constituents for the last three satellite altimetry missions.

Tidal Com-Ponent	Tidal period (hours)	Aliased period (days)		
		Geosat (17 days)	ERS1 (35 days)	T/P (10 days)
M_2	12.42	317	95	62
S_2	12.00	169	∞	59
N_2	12.67	52	97	50
K_2	11.97	88	183	87
K_1	23.93	176	365	173
O_1	25.82	113	75	46
P_1	24.07	4466	365	89
Q_1	26.87	74	133	69

The T/P empirically derived solutions rely heavily on averaging of the data over areas of about a 3° radius. This averaging is necessary to overcome the tidal aliasing constraints. Indeed, a detailed analysis of these solutions reveals that they are a little noisy spatially. Their accuracy is also limited over areas where tides are spatially complex. One way to reduce these limitations is to use the more sophisticated methods developed and tested before the advent of T/P. An application has been realized successfully on the basis of the represent method, assimilating most of the cross-over data from 38 T/P cycles (8). An inverse solution has been computed on a 0.7° by 0.7° grid for a direct determination of the four principal tidal constituents M_2, S_2,

K_1 and O_1 (9) . These solutions are computed totally independently of any previously known tidal solution.

With longer T/P observations, signal-noise ratio will be improved and aliasing problems will be removed. It is expected that the signal-noise ratio will be reduced by a factor of 1.4 to 1.5 , which approaches the limits of tidal analysis methods (10 ,11) . The combination of high – quality altimetry and an increase in computer resources (making it possible to increase the physical realism and the resolution of the numerical models) all point toward further improvements in tidal modeling in the next few years. The tidal solutions will benefit many fields of geodesy, geophysics, oceanography, and space technology. Using the new hydrodynamic models will also supply barotropic tidal currents in the deep ocean and shallow seas, with high resolution over continental shelves . Therefore they will benefit environmental and engineering investigations along coasts and marginal seas.

Tidal Data in the Gulf of Thailand

The gulf of Thailand, is an important region for the study of international sea-waters. The territorial waters in Thailand are mainly under the influence of the moon and the topographical features of the coast.

Tidal observations began in Thailand in 1904 when a staff gauge was installed and regular visual readings were recorded (12). A German made , automatic tide gauge began operation in September 1910 at Kao Lak (11° 47′ 42″ N, 99° 48′ 58″ E) Prachuab-kireekan on the west coast of the Gulf of Thailand. The first calculation of a mean sea level (MSL) covered the period from October 10, 1910 to April 30,1911.

A bench mark B.M.A, the first one in Thailand, was then established on shore at Kao-Lak. This bench mark was 1.4439 meters above the mean sea level measured.

In October 1915, the data collected from October 10, 1915 were used to recalculate the MSL. The value of the MSL obtained was 0.0038 meters lower than the previous one. Therefore, 0.0038 meters were added to the height of the bench mark. Since it was known that tidal ranges along Thailand 's coast did not exceed 5.0 meters, the tidal datum was set at 2.5 meters below the MSL (Figure 1.1).

In 1953 the Hydrographic Department acquired a tide prediction machine and it became possible to extend the predictions to cover various locations along both the Gulf of Thailand coast and the Andaman Sea coast.

From 1977 to 1995, the daily predictions of hourly heights of the tide for all stations were calculated by computer. Beginning in 1997 , the hourly heights of the tide at an additional seven stations have been predicted.

At the present time, tidal analysis and predictions of the Hydrographic Department are based on calculations made by the Harmonic Method (13). The calculations are done as follow.

To find height for a given time.

If t_1 and h_1 denote the time and height of tide (high or low) immediately preceding time t , t_2 and h_2 denote the height of tide (high or low) immediately following, then the height h at time t is given by the following formula;

$$h = h_1 + [(h_2 - h_1) * (\cos A + 1)]/2$$

where $A = \pi * [(t - t_1)/(t_2 - t_1) + 1]$ radians.

note 1 : On falling tide, $(h_2 - h_1)$ will be negative.

note 2 : t , t_1 and t_2 are in decimal of hour.

To find time for a given height.

With t_1, h_1, t_2 and h_2 defined as above, the intermediate time t when the tide is at a given height h, can be calculated from the following formula :

$$t = t_1 + [(t_2 - t_1) * ((A/\pi) - 1)]$$

where $A = 2\pi - \cos^{-1}[2 * (h - h_1)/(h_2 - h_1) - 1]$ radians

note 1 : On falling tide $(h - h_1)$ and $(h_2 - h_1)$ will be negative.

note 2 : t , t_1 and t_2 are in decimal of hour.

note 3 : It is presumed that the range of the $\cos^{-1}$ function is $(0, \pi)$

Variations in the flow of the rivers and abnormal weather conditions are factors which may affect the accuracy of such predictions to some minor extent.

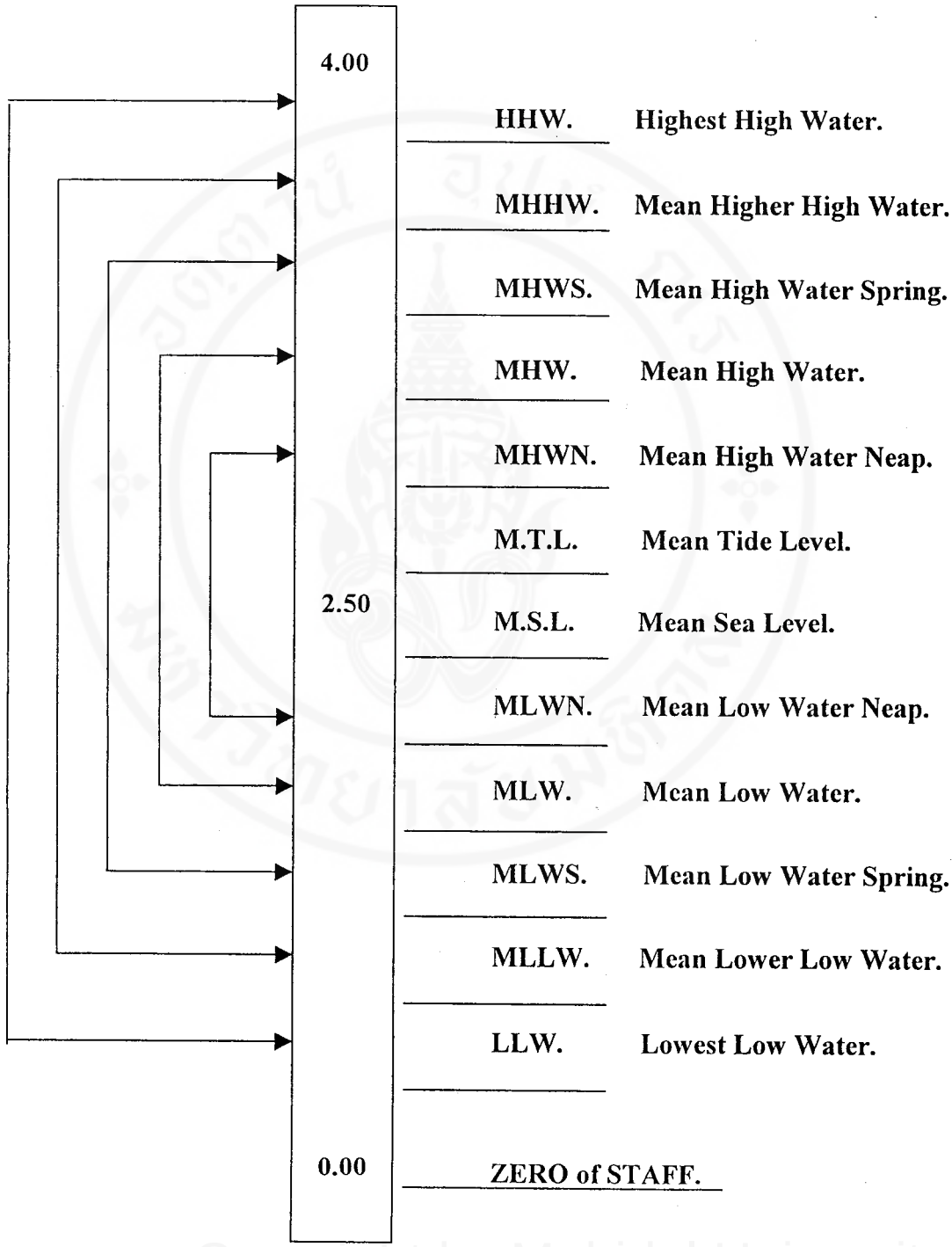

Figure 1.1 Chart of Height Level of Tidal Datum

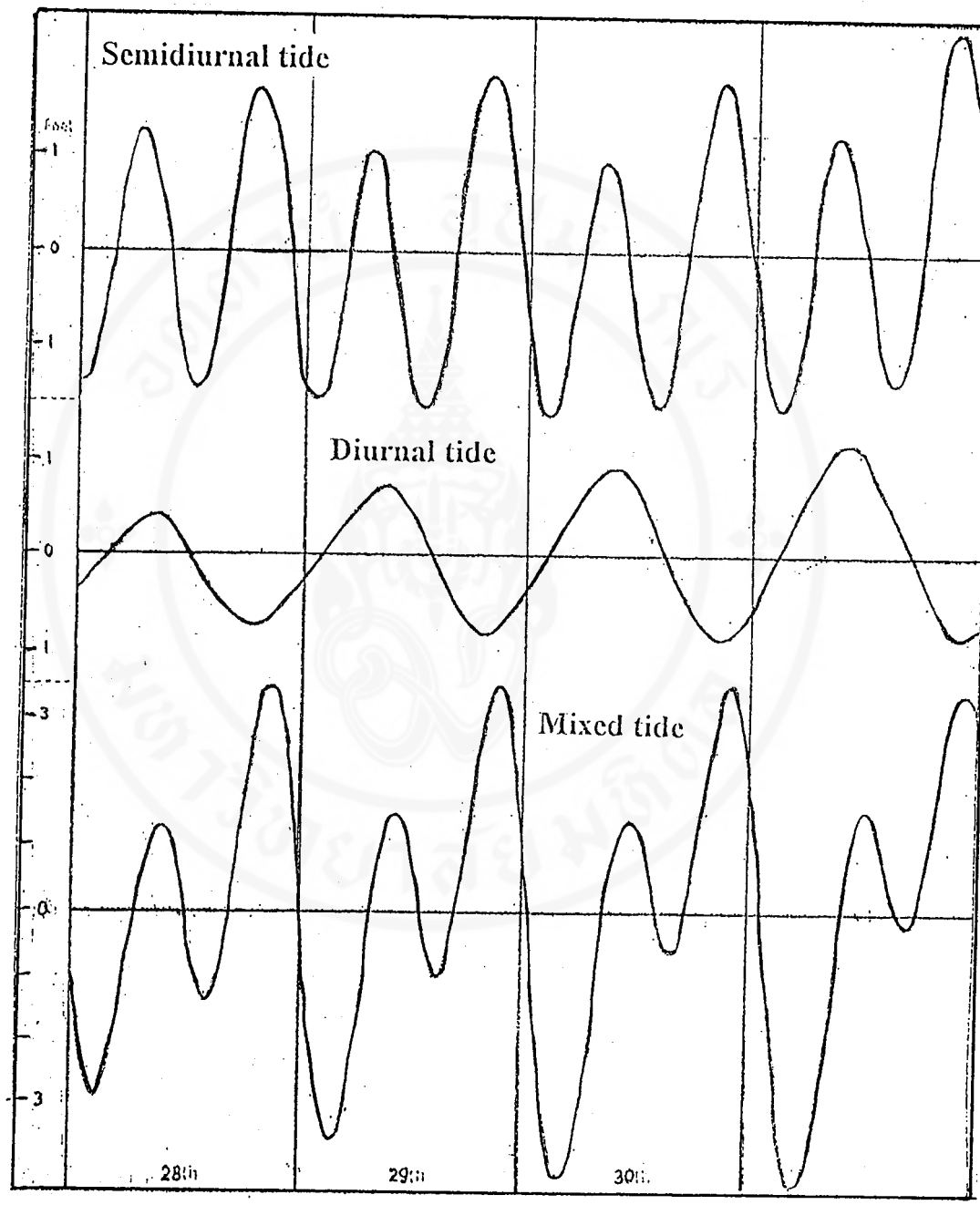

Figure 1.2 Chart of Type of Tide

Tidal Patterns

Before the development of appropriate instrumentation, sea-level observations were confined to the coast and were not very accurate. Regular water movements are seen as both the vertical rise and fall of sea-level, and the to and from movements of the water currents. Levels at more than 3000 sites have been analysed and their tidal characteristics are published by the International Hydrographic Organization in Monaco. Less elaborate analyses for around 1000 further sites are available in published Tide Tables.

The two main tidal features of any sea-level record are the range, measured as the height between successive high and low levels, and the period, the time between one high (or low) level and next high (or low) level. The tidal responses of the ocean to the forcing of the moon and sun are very complicated and both of these tidal features vary greatly from one site to another.

In most of the world's oceans the dominant tidal pattern is similar to that shown in Figure 1.2 . Each tidal cycle takes an average of 12 hours 25 minutes, so that two tidal cycles occur for each transit of the moon (every 24 hours 50 minutes). Because each tidal cycle occupies roughly half of a day, this type of tide is called semidiurnal. Semidiurnal tides have a range which typically increases and decreases cyclically over a fourteen-day period. The maximum ranges, called spring tides, occur a few days after both new and full moons (syzygy, when the moon, earth and sun are in lime), whereas the minimum ranges, called neap tides, occur shortly after the times of the first and last quarters (lunar quadrature). The relationship between tidal ranges and the phase of the moon is due to the additional tide-raising attraction of the sun, which reinforces the moon's tides at syzygy, but reduces them at quadrature.

When the moon is at its maximum distance from the earth, known as lunar apogee, semidiurnal tidal ranges are less than when the moon is at its nearest approach, known as lunar perigee. This cycle in the moon's motion is repeated every 27.55 solar days, Maximum semidiurnal ranges occur when spring tides (syzygy) coincide with lunar perigee (Wood, 1986), whereas minimum semidiurnal ranges occur when neap tides (quadrature) coincide with lunar apogee. Semidiurnal tidal ranges increase and decrease at roughly the same time everywhere, but there are significant local differences.

Figure 1.2 . shows that at certain times in the lunar month successive high-water levels of the semidiurnal tides are alternately higher and lower than the average. This behaviour is also observed for the low-water levels, the differences being most pronounced when the moon's declination north and south of the equator is greatest. The differences can be accounted for by a small additional tide with a period close to one day, which adds to one high water level but subtracts from the next one. Because this tide has a period close to one day, it is called a diurnal tide.

The diurnal tides are similar in magnitude to the semidiurnal tides. The diurnal tides are most important when the moon's declination is greatest, but they reduce to zero when the moon has zero declination. i.e., when it is passing through the equatorial plane. This is because the effect of declination is to produce an asymmetry between the two high and the two low-water levels of each day. The semidiurnal tides are most important after new and full moon; but unlike the diurnal tides, they do not reduce to zero range, being only partly reduced during the period of neap tides.

All tides have both semidiurnal and diurnal components. In semidiurnal tides the relative importance of the semidiurnal component is greater than that of the diurnal component. Similarly, in diurnal tides the relative importance of the diurnal component is greater than that of the semidiurnal component. When both components have similar magnitude, the tide is called a mixed tide.

More generally it is enough to define the semidiurnal tides as having two high (or two low) waters in a period of a lunar day with almost equal heights, and to define mixed tides as having two high (or two low) waters in a period of a lunar day with clearly unequal heights. But for technical purposes we must have some better criteria for the different types of tide. The relative importance of the diurnal and semidiurnal tidal constituents is sometimes expressed in terms of a Form Factor (14) :

$$F = \frac{K_1 + O_1}{M_2 + S_2} ,$$

where K_1 and O_1 are amplitudes of the diurnal component

M_2 and S_2 are amplitudes of the semidiurnal component.

The tides may be roughly classified as follows:

F	=	0 to 0.25	semidiurnal form
F	=	0.25 to 1.50	mixed, mainly semidiurnal
F	=	1.50 to 3.00	mixed, mainly diurnal
F	=	greater than 3.0	diurnal form

A more exact definition of the tidal regime in terms of the relative importance of the diurnal and semidiurnal components must involve the ratios of the total variance in each tidal type, but at best this type of description is only an approximate representation of the full tidal characteristics.

Objective

To develop a new method to yield accurate and precise predictions of hourly heights of the tide (mixed type) (Figure 1.2) and to study the behavior of tides (mixed type) at different locations. Analyze and compare the accuracy of solutions obtained from data assimilation models and empirical by Least Square best fits models.

Scope and Source of Data

There are three types of tides in the Gulf of Thailand , diurnal , semidiurnal and mixed type. It should be noted that there is a marked difference in the characteristics of the tide at each locality in the territorial water of Thailand.

1. Data for the study is for tides of mixed type.
2. Sources of data are the coast of Pak Nam Tachin , Ko Sichang and HuaHin in 1996 Figure 1.3 and Table 1.2 .
3. Tide Stations are Harbour Department , Port Authority of Thailand and Hydrographic Department.

Table 1.2 Location of Project Tide Stations

No	Code	Station Name	Latitude	Longitude
1.	HH	Hua Hin	12°34′22″ N	99°57′48″ E
2.	TCH	Pak Nam Tachin	13°30′36″ N	100°16′40″ E
3.	KSC	Ko Sichang	13°09′30″ N	100°48′41″ E

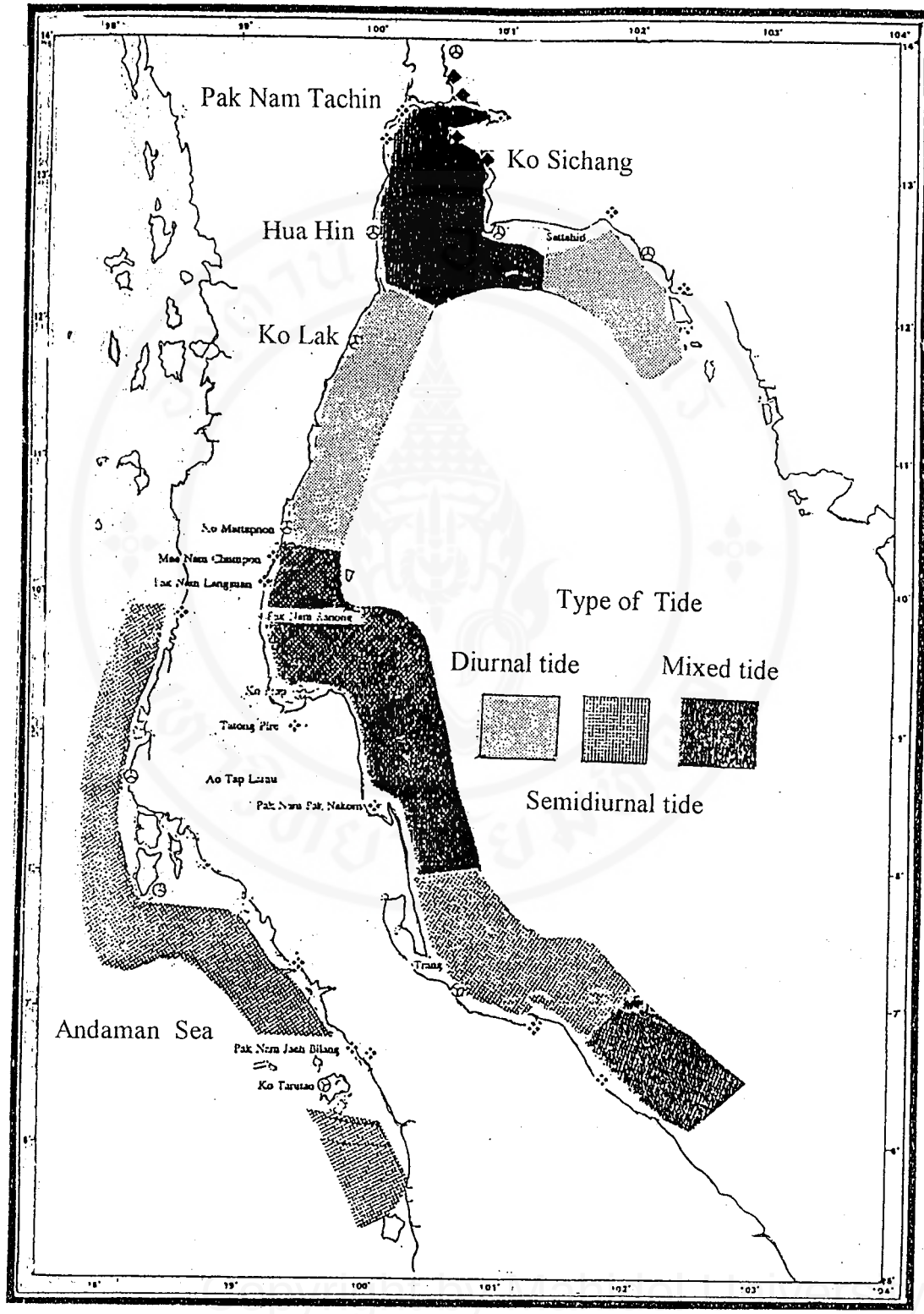

Figure 1.3 Chart of the tide stations.

In this thesis, we consider data assimilation methods (15). Data assimilation is the name given to the process of combining a physical model with observational data to provide a state analysis of the system which is better than that be obtainable using just the data or physical model alone. Data assimilation methods for tidal analysis combine a model with data to obtain a better estimate of the ocean state. The methods can be divided into sequential methods and model trajectory methods. Sequential methods combine model and data at given times, usually when sufficient new observations have been collected. Once the analysis step is carried out for a given time, a forward integration is made to the next assimilation time using the results of the analysis as initial conditions for the model. The process is repeated. In the model-trajectory approach, data gathered during a time interval are used to obtain the model trajectory that best fits the data over the whole interval. If the model is assumed to be perfect, the model trajectory is determined by its initial and/or boundary conditions, and so the problem reduces to a search for the optimal values of these "control variables". For the subsequent time interval, the model state at the beginning is modified to the new data, and the process is repeated.

Over recent years the increased motivation for the use of data assimilation methods in oceanography has been due to improvements of the observing systems, advances in data assimilation techniques and ocean modeling.

In Chapter II, we discuss some theoretical background for the data assimilation technique. We first discuss the physical theory for constraint equations which come from basic hydrodynamics. The constraint equations fall into three categories : *Kinematical Equations* , *The Equation of Continuity* and *The Bernoulli Equation*. We

then discuss a Lagrange Multipliers method which the existence of a parametric representation and then deriving necessary conditions for there to be extreme point for a function restricted to a parametrized curve or surface.

In Chapter III, we apply the theoretical background of Chapter II to solve the problem. We discuss the method of data assimilation. In model-trajectory method that consist the following step : raw data interpolation because of break down in the record, defining the modeled state and the model constraint equations from the basis of hydrodynamics and finding a stationary point of Lagrange Multipliers and solving the systems of equations on a computer.

In Chapter IV, from methodology in Chapter III we will discuss and show the result of the data assimilation method and the best least square fit method by value of parameters from tables and consider characteristics of tide from graphs. We compare models by the sum square error.

Finally, Chapter V , we will conclude the success of models of mixed tide type from result in Chapter IV , including discuss to problem in each method.

CHAPTER II

THEORETICAL BACKGROUND

Before the raw data recorded by the instrumental system is ready for scientific analysis it must go through a process of checking and preparation known as data reduction (UNESCO, 1985b). The recorded data may be in the form of a chart recording such as that shown in Figure 2.1, a trace on photographic film, a punched paper tape, or a digital signal stored on magnetic tape. This data must be read either by eye or by a mechanical translator, checked for recording errors, and adjusted for calibration factors and for control clocks running fast or slow. Gaps are interpolated if necessary before the data is filtered to obtain values at standard times. Usually, but not invariably, oceanographic changes with a strong tidal component are presented for analysis in the form of hourly values, on the hour, either in local time or in Greenwich Mean Time. When the data has been processed, it is highly desirable that it is preserved with proper documentation in a permanent computer-based data bank.

In the following sections, Data assimilation methods , Basic hydrodynamics and Lagrange multipliers are described.

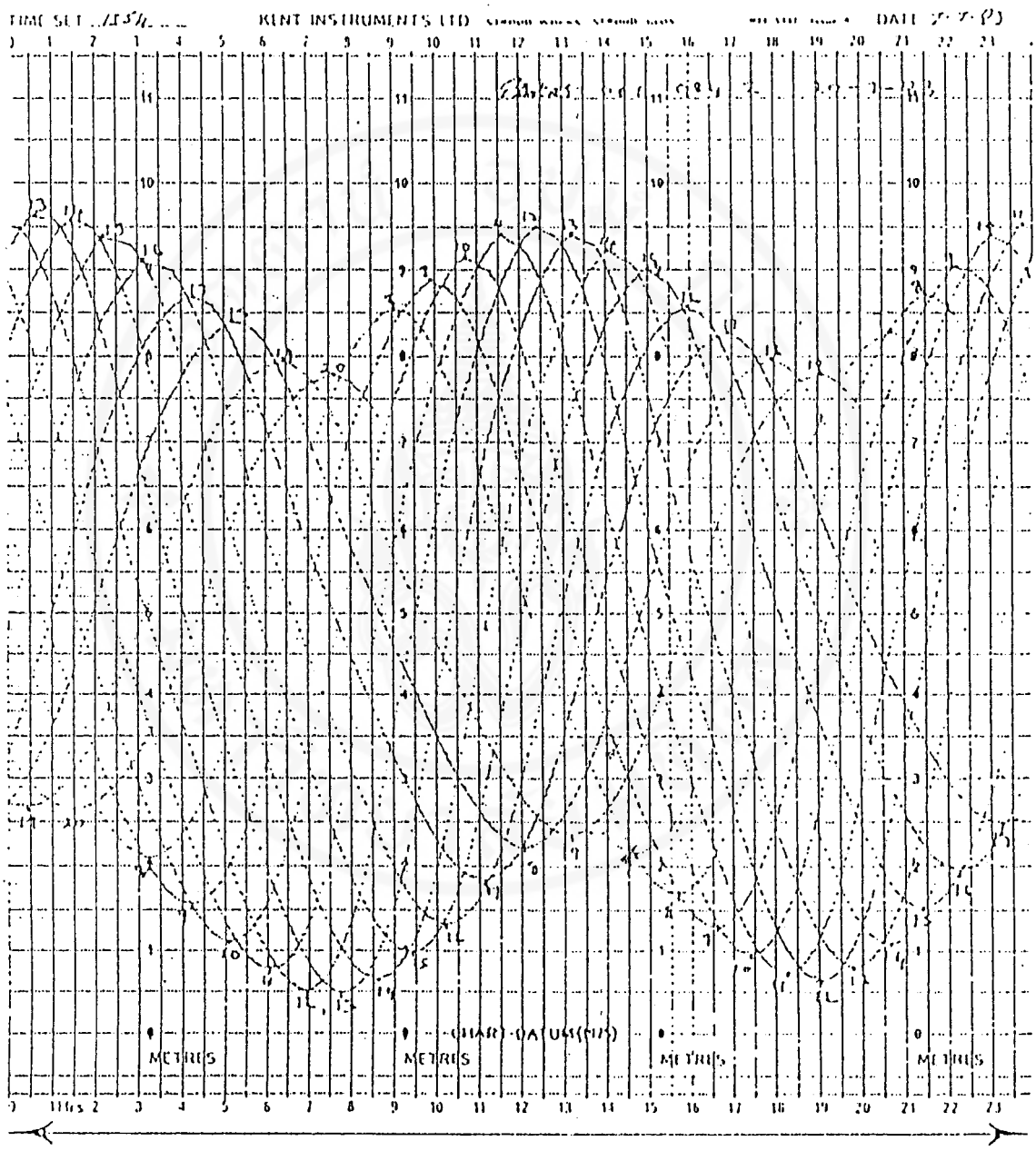

Figure 2.1 Example of a chart recorded data.

Data Assimilation Methods

Data assimilation methods combine a theoretical model with data to obtain an estimate of the ocean state than could be obtained either from empirical data analysis alone or from a physical model alone. The data assimilation techniques can, in a broad sense, be divided into sequential and model trajectory methods. Sequential methods combine model and data at given times (this is called the analysis), usually when sufficient new observations have been collected. Once the analysis is carried out for that time, a forward integration is made to the next assimilation time using the analysis as initial conditions for the model, and the process is then repeated. In the model-trajectory approach, data gathered during a time interval are fitted to a model, and the best model trajectory that fits the data over the whole interval is calculated. If the model is assumed to be perfect, the model trajectory is determined by its initial and / or boundary conditions, and so the problem reduces to a search for the optimal values of these 'control variables'. For the subsequent time interval, the model state at the beginning is modified to fit the new data, and the process is repeated.

In the model-trajectory method , variational method is used for trajectory analysis. These variational methods were first proposed in principle by Sasaki (1970), and they were subsequently given a large practical boost by the work of Lewis and Derber (1985), Le Dimet and Talagrand (1986), and Thacker and Long (1987). At the heart of the variational approach is the minimization of some number defined as a "cost function", or "objective function", J, which measures the difference between the modeled state , or time trajectory of the system, and the observations. The observations are usually distributed in space and time. To find the solution to the

model equations which most closely fits observations over some time interval, the cost function is minimized with respect to free parameters.

A typical cost function used is of the form

$$J = \sum_{t=1}^{n} \left(h_{obs}(t) - h_{pre}(t)\right)^2 \quad , \tag{2.1}$$

where $h(t)$ denoted the height of tide level at any time,

$h_{obs}(t)$ comes from all data observations and $h_{pre}(t)$ is a state model of the form

$$h_{pre}(t) \quad = \quad a_0 + a_1 \sin t + a_2 \cos t \quad , \tag{2.2}$$

with a_0, a_1, a_2 are free parameters in the model. The cost function then becomes

$$J = \sum_{t=1}^{n} \left[h_{obs}(t) - \left(a_0 + a_1 \sin t + a_2 \cos t\right)\right]^2. \tag{2.3}$$

Now not all of the free parameters in equation (2.3) are independent, since the model must satisfy the three physical constraint equations. Therefore, minimizing J with respect to the free parameters is a constrained minimization problem. A constrained minimization problem can be posed as an unconstrained problem by introducing Lagrange multipliers λ. The constrained minimum of J is then obtained by finding the stationary points of the Lagrangian L defined by

$$L \quad = \quad J + \sum_{t=1}^{n} \lambda_t R_t \quad , \tag{2.4}$$

where R_t is residual functions which come from basic hydrodynamics.

From equation (2.4), that there are as many Lagrange multipliers as there are hydrodynamic constraint equations and integrals over space and time as well.

The advance by Le Dimet and Talagrand was to show that the unconstrained gradient of L with respect to all the free parameters could be obtained from one single integration of the adjoint of the equations of motion and that it was not necessary to vary each of the free parameters, separately.

A practical way to solve (2.4) for real problems has been given by Thacker and Long (1988). They proposed that from the start one write down the Lagrangian, not in its analytic form, but in its numerical (finite difference) form, with a Lagrange multiplier for every time step of the finite difference equations. If one now differentiates the analogue of (2.4) with respect to t , one obtains equations for the Lagrange multipliers in a finite difference form which are consistent with the original equations of motion. (The apparent analogue of using the analytic form of the adjoint equations to be satisfied by λ and then finite differencing those equations can lead to inconsistencies if the latter step is not done correctly.) The adjoint model program code is needed but it has been recognized that for a linearized model the adjoint is really just running the model, in some sense, backwards using the transpose. This means that in principle one could generate the adjoint by first linearizing the model then taking the transpose of every model statement in reverse order; work which could be done by a computer. Considerable progress has recently been made in automatic adjoint generators (Geiring and Kaminski 1995).

Basic Hydrodynamics

The residual functions in (2.4) are constraint equations which come from the basic equations of the hydrodynamics of an ideal (nonviscous) fluid. These equations fall into three categories : (1) they are essentially kinematical in nature; (2) an

equation expresses the conservation of mass when a fluid moves, the *equation of continuity* ; (3) a dynamical equation, *Bernoulli's equation*, summarizes the application of Newton's second law to fluids, in particular to the irrotational motion of an incompressible liquid , detail as follows.

1. Kinematical Equations

There exist two equivalent ways of describing a fluid when it is in motion. In the *eulerian method* we describe some aspect of the fluid in terms of what takes place at a fixed point $\boldsymbol{r}_0 = (x_0, y_0, z_0)$, as the fluid flows by. We are thus continually observing new particles as they pass the point of observation. In the *Lagrangian method* we pick out a single particle of the fluid and follow it along as it partakes of the fluid motion. We can then describe the same aspect of the fluid that was of interest before but now in terms of what happens to the fluid in the immediate vicinity of a specific moving particle. Let us see how the two viewpoints are related so far as time rates of change are concerned.

Let $F(x, y, z, t)$ stand for some (scalar) property of the fluid that may be of interest, e.g., its density , or one of the components of its velocity. If we stay at a fixed point $\boldsymbol{r}_0$, we can observe F as a function of time and can therefore calculate the rate of change $\partial F/\partial t$ at this point. From this limited knowledge of F we have no way of knowing, as yet, how F changes with time if we stay with a particular particle and follow it along as it passes through the point at $\boldsymbol{r}_0$. To find this Lagrangian rate of change we need to relate the value of F at $\boldsymbol{r}_0$ at time t_0 to its value at a neighboring point $\boldsymbol{r}_0 + d\boldsymbol{l}$ at time $t_0 + dt$, where $d\boldsymbol{l} = \boldsymbol{v}\, dt$ is a small displacement along the flow

line passing through the point at $\boldsymbol{r}_0$. Now $F_0 \equiv F(x_0, y_0, z_0, t_0)$ represents F at position $\boldsymbol{r}_0$, time t_0 and $\boldsymbol{v}$ denotes fluid velocity. When a particle at this point at the time t_0 arrives at the neighboring point at the time $t_0 + dt$ the function F has the value become

$$F = F(x_0 + d\xi, y_0 + d\eta, z_0 + d\zeta, t_0 + dt) \quad \text{or}$$

$$F = F_0 + \left(\frac{\partial F}{\partial x}\right)_0 d\xi + \left(\frac{\partial F}{\partial y}\right)_0 d\eta + \left(\frac{\partial F}{\partial z}\right)_0 d\zeta + \left(\frac{\partial F}{\partial t}\right)_0 dt . \qquad (2.5)$$

The total increment in F is therefore

$$dF = \left(\frac{\partial F}{\partial x}\right)_0 d\xi + \left(\frac{\partial F}{\partial y}\right)_0 d\eta + \left(\frac{\partial F}{\partial z}\right)_0 d\zeta + \left(\frac{\partial F}{\partial t}\right)_0 dt . \qquad (2.6)$$

Hence rate of change of F with respect to t from in the lagrangian viewpoint is

$$\frac{dF}{dt} = \left(\frac{\partial F}{\partial x}\right)_0 \frac{\partial \xi}{\partial t} + \left(\frac{\partial F}{\partial y}\right)_0 \frac{\partial \eta}{\partial t} + \left(\frac{\partial F}{\partial z}\right)_0 \frac{\partial \zeta}{\partial t} + \left(\frac{\partial F}{\partial t}\right)_0 , \qquad (2.7)$$

which may be more compactly written as

$$\frac{dF}{dt} = \boldsymbol{v} \cdot \nabla F + \frac{\partial F}{\partial t} , \qquad (2.8)$$

where gradient operation $\nabla = \mathbf{i}\frac{\partial}{\partial x} + \mathbf{j}\frac{\partial}{\partial y} + \mathbf{k}\frac{\partial}{\partial z}$ and

velocity of fluid $\boldsymbol{v} = \mathbf{i}\frac{\partial \xi}{\partial t} + \mathbf{j}\frac{\partial \eta}{\partial t} + \mathbf{k}\frac{\partial \zeta}{\partial t}$

Although we calculated (2.8) at a particular point and time, both position and time can be arbitrary chosen ; thus (2.8) constitutes a general kinematical relation that always holds for a fluid. And F is used to represent may be the density ρ of a compressible fluid or velocity of the fluid and the three component scalar equations are then combined into a single vector equation which is describe by the differential equation given as

$$\frac{d\boldsymbol{v}}{dt} = \boldsymbol{v}\cdot\nabla\boldsymbol{v} + \frac{\partial\boldsymbol{v}}{\partial t} \qquad (2.9)$$

Here $\frac{d\boldsymbol{v}}{dt}$ is the vector acceleration of the fluid at any point, which we need when we apply Newton's law to relate force fields to the acceleration of the fluid. If the fluid flow is steady, then $\frac{\partial\boldsymbol{v}}{\partial t} = 0$. However, there can still exist an acceleration of the fluid , $\boldsymbol{v}\cdot\nabla\boldsymbol{v}$, resulting from a dependence of $\boldsymbol{v}$ on position. The average angular velocity ω of the fluid in the vicinity of any point to the linear velocity $\boldsymbol{v}$ of the fluid is defined as

$$\omega = \tfrac{1}{2}\boldsymbol{curl}\,\boldsymbol{v} = \tfrac{1}{2}\nabla\times\boldsymbol{v}\,. \qquad (2.10)$$

In discussing waves on the surface of a liquid (as well as many other problems in hydrodynamics), it is customary to assume that the liquid motion is irrotational ,which means that the curl of $\boldsymbol{v}$ vanishes everywhere. This assumption in effect means that we are not interested in eddies, or vortices, which, when once set up in an ideal fluid, persist forever due to the conservation of angular momentum. (In real fluids vortices die out because of viscosity in the fluid, as illustrated by the behavior of smoke rings.)

The vanishing of the curl of $\boldsymbol{v}$ is a necessary and sufficient condition that $\boldsymbol{v}$ can be derived from a scalar velocity potential ϕ ,

$$\boldsymbol{v} = -\nabla\phi \quad , \tag{2.11}$$

where $\phi = \phi(x, y, z, t)$. As we shall see later , the velocity potential is almost indispensable for discussing waves on a liquid surface.

2. The Equation of Continuity

We have already pointed out that the equation of continuity expresses the conservation of the mass of a fluid. To obtain an equation embodying this idea, we compute the net entry of fluid mass into an element of volume $\Delta x\Delta y\Delta z$ in time Δt and equate it to the net increase in mass within the element. Now the quantity $\rho\boldsymbol{v}$ is the (vector) mass flow of the fluid, where $\boldsymbol{v} = \mathbf{i}v_x + \mathbf{j}v_y + \mathbf{k}v_z$ is the velocity of the fluid and ρ its density, both of which may be functions of position and time. The mass entering the element through the face $OBEC$ (see Fig. 2.2) in time Δt is $\rho v_x \Delta y\Delta z\Delta t$, and that leaving face $ADGF$ is

$$\left(\rho v_x + \frac{\partial}{\partial x}(\rho v_x)\Delta x\right)\Delta y\Delta z\Delta t \, .$$

Hence the net amount of mass entering the element in the x direction in time Δt is $-\frac{\partial}{\partial x}(\rho v_x)\Delta x\Delta y\Delta z\Delta t$, with similar expressions for the y and z directions. The total influx of mass is

$$\Delta M = -\left(\frac{\partial}{\partial x}\rho v_x + \frac{\partial}{\partial y}\rho v_y + \frac{\partial}{\partial z}\rho v_z\right)\Delta x\Delta y\Delta z\Delta t \, . \tag{2.12}$$

On dividing by $\Delta x \Delta y \Delta z \Delta t$, passing to the limit $\Delta x \to 0$, etc. and identifying the quantity in parentheses in (2.12) as the divergence of the mass flow ρv, we obtain the *equation of continuity.*

$$\frac{\partial \rho}{\partial t} = -\text{div}\,(\rho v) = -\nabla \cdot (\rho v) \quad . \tag{2.13}$$

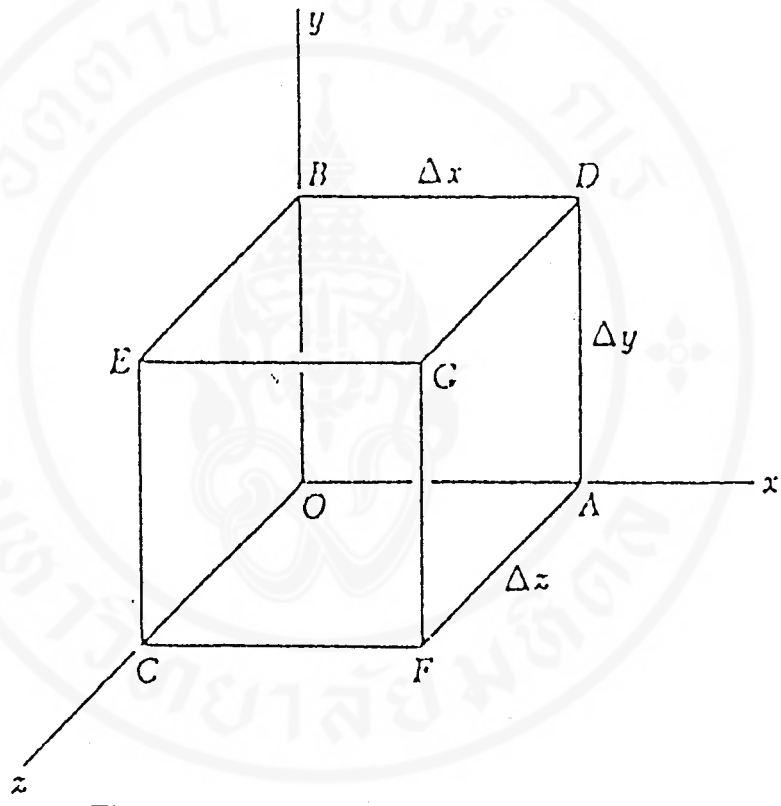

Figure 2.2 Element of volume in a fluid.

In the case of an incompressible fluid, the density ρ is a constant. The equation of continuity (2.13) then becomes

$$\nabla \cdot v = 0. \tag{2.14}$$

Substituting $v = -\nabla \phi$ into equation (2.14) , we obtain the *Laplace's equation*

$$\nabla \cdot \nabla \phi = 0. \tag{2.15}$$

3. The Bernoulli Equation

Let us now apply Newton's second law to the mass $\rho\Delta\tau$ in an element of volume $\Delta\tau$ of a fluid. The net force , F , acting on an element to consist of an external body force due to gravitational acceleration , g , and an internal force which arising from a variation of the pressure from point to point in the fluid. An internal force is given by

$$\Delta F_i = -\nabla P \ \Delta\tau, \tag{2.16}$$

where ∇P is the pressure gradient. While the external force due to gravity is defined by

$$\Delta F_e = \rho g \Delta\tau = -\rho \nabla\Omega \Delta\tau, \tag{2.17}$$

where Ω is the gravitational potential energy per unit mass such that $g = -\nabla\Omega$. (For instance, if the y-axis is directed upward , then $\Omega = gy$, and $g = -\mathbf{j}g$.) Newton's second law therefore states that

$$-\rho\nabla\Omega - \nabla P = \rho\frac{dv}{dt}. \tag{2.18}$$

We now introduce (2.9) into the RHS of equation (2.18) to express the (lagrangian) acceleration of the fluid motion. We then have

$$-\nabla\Omega - \frac{1}{\rho}\nabla P = \frac{\partial v}{\partial t} + v\cdot\nabla v. \tag{2.19}$$

Under assumption that the liquid motion is irrotational , i.e. $\nabla\times v = 0$ and $v = -\nabla\phi$,we then have $\nabla\times v = 0$,

$$(\nabla\times v)\times v = (v\cdot\nabla)v - \nabla(v\cdot v) = 0,$$

so that

$$\boldsymbol{v}\cdot\nabla\boldsymbol{v} = (\nabla\boldsymbol{v})\cdot\boldsymbol{v} = \nabla\left(\tfrac{1}{2}v^2\right). \tag{2.20}$$

and obtain

$$\frac{\partial \boldsymbol{v}}{\partial t} = -\nabla\frac{\partial\phi}{\partial t}, \tag{2.21}$$

Substituting equations (2.20) and (2.21) into (2.19) yields the Bernoulli equation

$$-\nabla\Omega-\frac{1}{\rho}\nabla P = -\nabla\frac{\partial\phi}{\partial t} + \nabla\left(\tfrac{1}{2}v^2\right). \tag{2.22}$$

Now we define the total difference, dU, as

$$dU = d\boldsymbol{r}\cdot\nabla U, \tag{2.23}$$

where $U(x,y,z,t)$ is any scalar function of position and time and $d\boldsymbol{r}$ is vector of displacement and introduce into equation (2.22). We then have

$$-d\Omega-\frac{1}{\rho}dP = -d\frac{\partial\phi}{\partial t} + d\left(\tfrac{1}{2}v^2\right), \tag{2.24}$$

Integrating (2.24) when ρ is constant , yields the fluid can be considered incompressible , then

$$\frac{P}{\rho}+\Omega+\tfrac{1}{2}v^2 = \frac{\partial\phi}{\partial t} + f(t). \tag{2.25}$$

where $f(t)$ is the constant of integration, which may be a function of time.

We refer to the integral (2.25) of the equation of motion as *Bernoulli's equation*, a name which is also used for the different forms that the equation takes when the limitations of irrotational motion and incompressibility are not placed on the fluid.

We shall use Bernoulli's equation as a connecting link between the boundary condition of a constant pressure at the surface of a liquid and the variables that describe the kinematical aspects of a surface wave.

Therefore the displacement velocity of the fluid at any position and time is given by

$$\begin{aligned} v_x &= \frac{\partial \xi}{\partial t} = -\frac{\partial \phi}{\partial x} \\ v_y &= \frac{\partial \eta}{\partial t} = -\frac{\partial \phi}{\partial y} \\ v_z &= \frac{\partial \zeta}{\partial t} = -\frac{\partial \phi}{\partial z} = 0. \end{aligned} \tag{2.26}$$

Lagrange Multipliers

Theorem. Lagrange multiplier method.

Let the function $\Re^n \xrightarrow{G} \Re^m$, $n > m$, be continuously differentiable and have coordinate functions $G_1, G_2, \ldots, G_m$. Suppose the equations

$$\begin{aligned} G_1(x_1, \ldots, x_n) &= 0 \\ G_2(x_1, \ldots, x_n) &= 0 \\ &\vdots \qquad\quad \vdots \\ G_m(x_1, \ldots, x_n) &= 0 \end{aligned}$$

implicitly define a surface S in $\Re^n$, and that at a point x_0 of S the matrix $G'(x_0)$ has some m columns linearly independent (16).

If x_0 is an extreme point of a differentiable function $\Re^n \xrightarrow{f} \Re$, when restricted to S, then x_0 is a critical point of the function

$$f + \lambda_1 G_1 + \lambda_2 G_2 + \ldots + \lambda_m G_m$$

for some constants $\lambda_1, \ldots, \lambda_m$.

CHAPTER III

METHODOLOGY

In this chapter we discuss the method of data assimilation. The techniques can be divided into sequential and model trajectory methods. For this thesis we use the model- trajectory methods in solving problem. In the model-trajectory approach, data gathered during a time interval are fitted, seeking the best model trajectory that fits the data over the whole interval. The process of the method is as follows ;

Step 1. Test raw data and interpolate the data for the error data observations because of break down in the record.

Step 2. Formulate the modeled state or time trajectory of the system and define 'cost function ' of ' objective function' , J, measuring the difference between the modeled state and observations.

Step 3. Define the model constraint equations from the basic equations of the hydrodynamics and input initial condition.

Step 4. A constrained minimum of J is then reduced to finding a stationary point of the Lagrangian L, (Lagrange Multipliers λ).

Step 5. A system of equations is then solved by computer program, we have a model of the mixed tide.

Diagram of the process of data assimilation is shown in figure 3.1

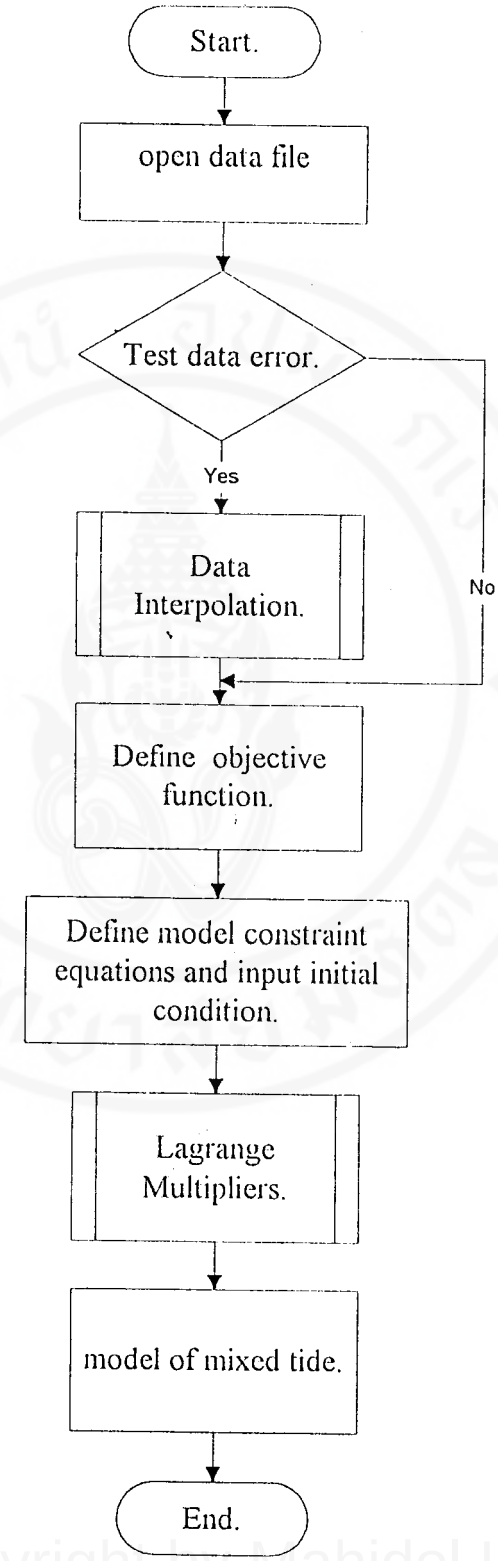

Figure 3.1 Diagram of the process of Data assimilation

Interpolation of Breaks in the Record

Since the time and height of tide vary day to day , observation data each station have error due to both instrument and observer. We must interpolate the incomplete data. Comfortable method is interpolation of time and height linearly type (17). In this thesis the mean value of data for 24 hours previous and after are used to interpolate, if value of data are out of range of possible value $[0,5]$. (Occurring from bad instrument or missing observation) ,we delete those data. Then we will calculate new data as

$$h(t) = \frac{h(t-24)+h(t+24)}{2} . \qquad (3.1)$$

If $h(t-24)$ or $h(t+24)$ are not in interval $[0\ ,\ 5]$ then we will calculate new data from

$$h(t) = \frac{h(t-48)+h(t+48)}{2} . \qquad (3.2)$$

For example. 3 days data at Hua-Hin station.

1	2	3	4	5	6	7	...	20	21	22	23	24	*date*
3.34	3.30	3.22	3.02	2.72	2.32	1.96	...	3.56	3.40	3.27	3.18	3.17	*210196*
3.19	3.20	9.99	9.99	9.99	9.99	9.99	...	9.99	9.99	9.99	3.08	2.94	*220196*
2.99	3.04	3.08	3.11	3.05	2.83	2.51	...	3.70	3.59	3.39	3.18	2.97	*230196*

Above example shows that there are 20 error values from 3rd hour to 22nd hour on Jan 22, 1996 . We will interpolate the height of tide level at 3rd hour , 4th hour , etc as follows : $h(3) = \frac{3.22+3.08}{2} = 3.15$,

$$h(4) = \frac{3.02+3.11}{2} = 3.065 \quad , \ \ldots.$$

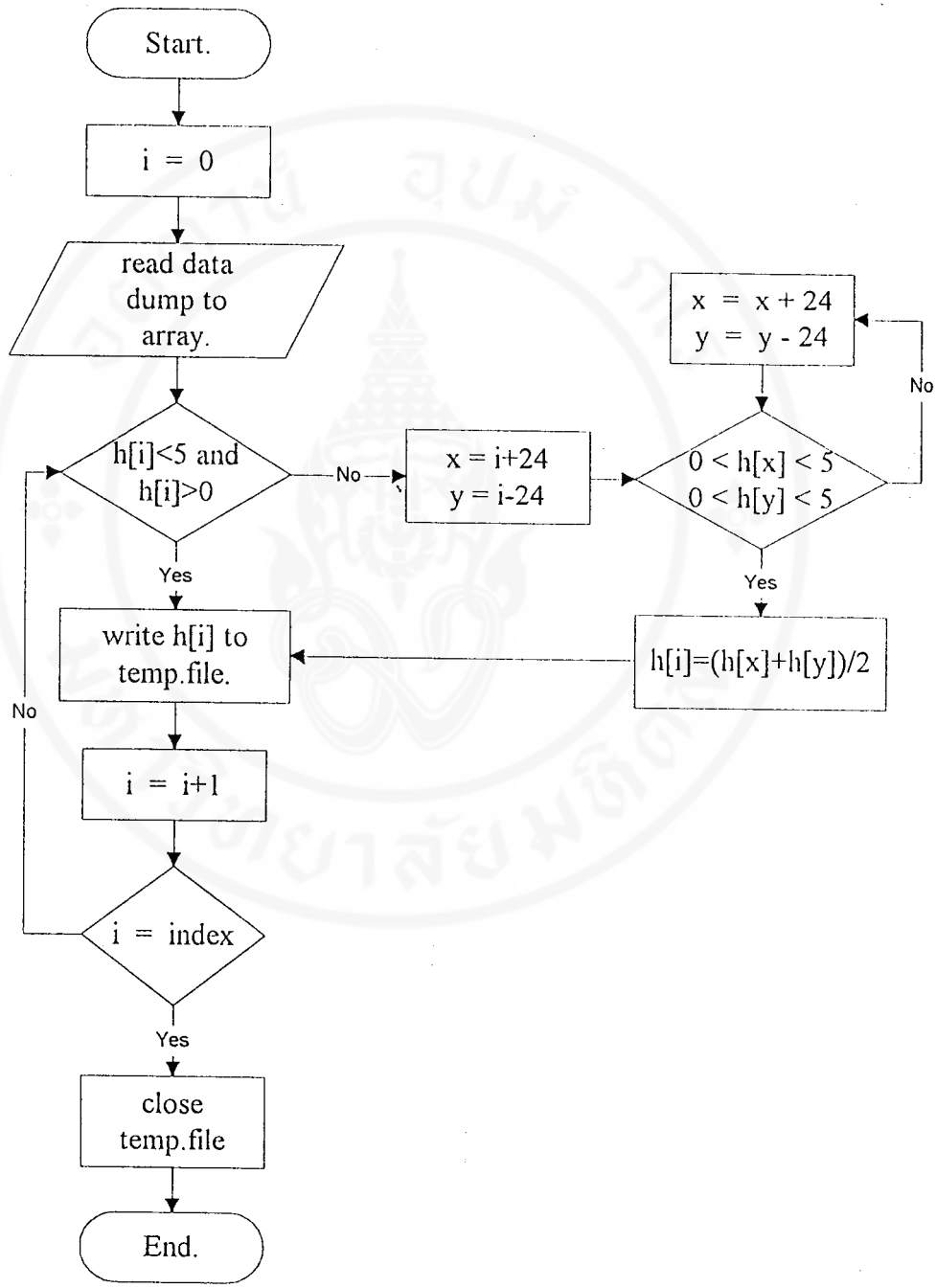

Figure 3.2 Chart of interpolation of break in the record

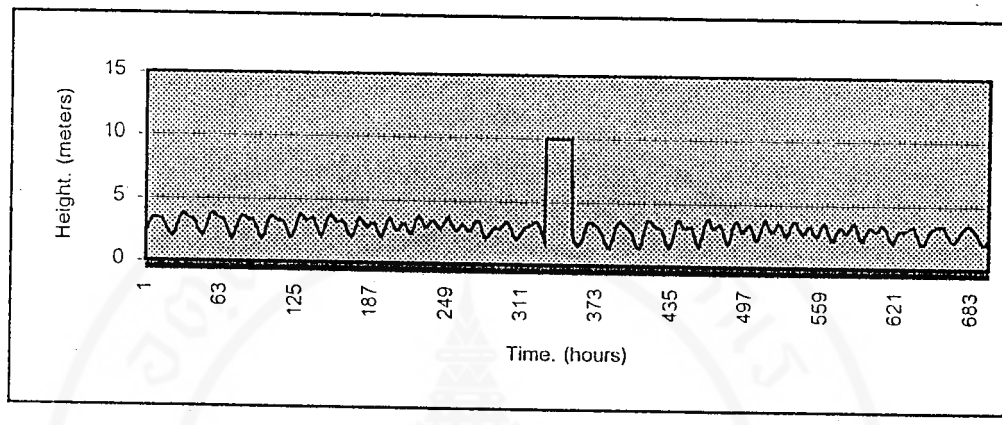

Figure 3.3 (a) Example of graph of error data observation

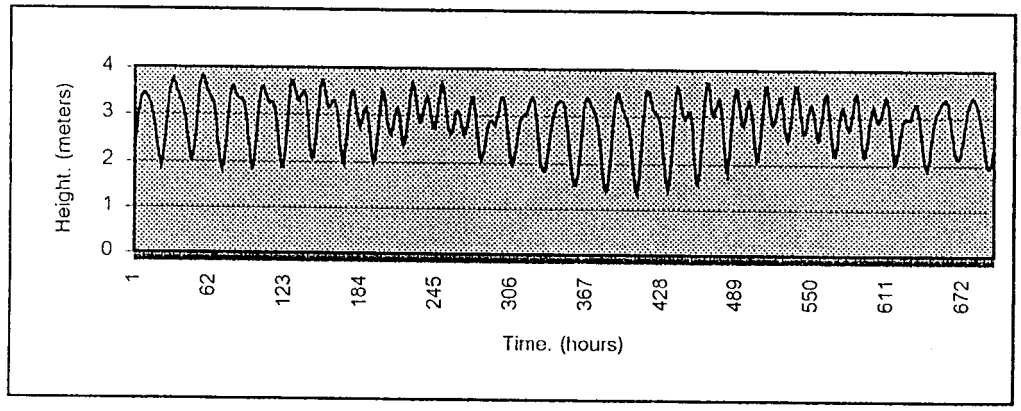

Figure 3.3 (b) Example of graph of data interpolation

Least Square Formulation.

The least squares method approach to this problem involves determining the best approximating curve giving an error which is the sum of the squares of the differences between the data observation which has been filtered and the model state of level-water. The constants a_0 , a_1 and a_2 must be found that minimize the least squares error :

$$E = \sum_{t=1}^{n} [h_{obs}(t) - a_0 - a_1 \sin t - a_2 \cos t]^2 \quad , \qquad (3.3)$$

where the model state is

$$h_{pre}(t) = a_0 + a_1 \sin t + a_2 \cos t .$$

Differentiate equation (3.3) with respect to a_0 , a_1 and a_2 then set all to zero, we obtain

$$\begin{aligned}
\frac{\partial E}{\partial a_0} &= 2\sum_{t=1}^{n} [h(t) - a_0 - a_1 \sin t - a_2 \cos t](-1) &= 0 \\
\frac{\partial E}{\partial a_1} &= 2\sum_{t=1}^{n} [h(t) - a_0 - a_1 \sin t - a_2 \cos t](-\sin t) &= 0 \qquad (3.4) \\
\frac{\partial E}{\partial a_2} &= 2\sum_{t=1}^{n} [h(t) - a_0 - a_1 \sin t - a_2 \cos t](-\cos t) &= 0
\end{aligned}$$

Using the distributive property of addition, the values a_0, a_1 and a_2 can be moved to outside the summations in (3.4). The normal equations there are given in (3.5)

$$
\begin{aligned}
a_0 n &+ a_1 \sum_{t=1}^{n} \sin t &+ a_2 \sum_{t=1}^{n} \cos t &= \sum_{t=1}^{n} h(t) \\
a_0 \sum_{t=1}^{n} \sin t &+ a_1 \sum_{t=1}^{n} \sin^2 t &+ a_2 \sum_{t=1}^{n} \sin t \cos t &= \sum_{t=1}^{n} h(t) \sin t \qquad (3.5) \\
a_0 \sum_{t=1}^{n} \cos t &+ a_1 \sum_{t=1}^{n} \sin t \cos t &+ a_2 \sum_{t=1}^{n} \cos^2 t &= \sum_{t=1}^{n} h(t) \cos t
\end{aligned}
$$

System of linear equation (3.5) can be written in matrix form as

$$
\begin{bmatrix}
n & \sum_{t=1}^{n} \sin t & \sum_{t=1}^{n} \cos t \\
\sum_{t=1}^{n} \sin t & \sum_{t=1}^{n} \sin^2 t & \sum_{t=1}^{n} \sin t \cos t \\
\sum_{t=1}^{n} \cos t & \sum_{t=1}^{n} \sin t \cos t & \sum_{t=1}^{n} \cos^2 t
\end{bmatrix}
\begin{bmatrix} a_0 \\ a_1 \\ a_2 \end{bmatrix}
=
\begin{bmatrix}
\sum_{t=1}^{n} h(t) \\
\sum_{t=1}^{n} h(t) \sin t \\
\sum_{t=1}^{n} h(t) \cos t
\end{bmatrix},
\qquad (3.6)
$$

which can be easily solved by program computer.

Data Assimilation Formulation.

We consider to process of data assimilation method by divide to be 2 parts : equation of motion which come from basic hydrodynamics and Lagrange multipliers which combine between objective function and physical constraints.

1. Equation of motion

In chapter II , we discussed to the basic equations of the hydrodynamics of fluid. Which can be classified into three categories: kinematical equations , the equation of continuity and the Bernoulli equation. For the Eulerian method, we use ξ, η and ζ notation to designate the components of the displacement. The displacement velocity of the fluid at any position and time is then

$$v_x = \frac{\partial \xi}{\partial t} = -\frac{\partial \phi}{\partial x} ,$$

$$v_y = \frac{\partial \eta}{\partial t} = -\frac{\partial \phi}{\partial y} .$$

At the bottom of the sea , the boundary condition of vanishing vertical velocity is

$$v_y = -\frac{\partial \phi}{\partial y} = 0 \qquad (y = 0), \tag{3.7}$$

At the sea surface , the pressure P_0 assumed to be constant.. We can turn this latter condition into a boundary condition on ϕ using Bernoulli's equation (2.25) but omitting the nonlinear term $\frac{1}{2}v^2$ for simplicity of analysis, The potential energy of unit mass of liquid at the surface when it has been displaced η_h in the vertical direction by the passage of a wave is evidently

$$\Omega = g(h + \eta_h). \tag{3.8}$$

Hence Bernoulli's equation at the surface of the water becomes

$$P_0 + \rho_0 g(h + \eta_h) = \rho_0 \frac{\partial \phi}{\partial t} + const \qquad (y = h), \tag{3.9}$$

where any time-dependent part of $f(t)$ has been absorbed in the as yet undetermined function $\frac{\partial \phi}{\partial t}$.

Equation (3.9) , basically , constitutes a relation between the variation in pressure at $y = h$ arising from the vertical displacement of the surface, the term $\rho_0 g \eta_h$, and the time derivative of the velocity potential, the term $\rho_0 \frac{\partial \phi}{\partial t}$. Here the variation in surface elevation gives rise to the (weak) elastic restoring force that replaces the (strong) elastic restoring force that exists for compressional waves in fluids.

If we now take a time derivative of (3.9) , treating P_0 as a constant and replacing $\frac{\partial \eta_h}{\partial t}$ by its equal $-\frac{\partial \phi}{\partial y}$, evaluated at $y = h$, we find that ϕ satisfies the boundary condition at the surface

$$v_y = -\frac{\partial \phi}{\partial y} = \frac{1}{g}\frac{\partial^2 \phi}{\partial t^2} \qquad (y = h). \qquad (3.10)$$

Once we have established how ϕ depends on position and time , Bernoulli ' s equation can be used to compute the pressure at any point in the liquid.

Our task is now to find a velocity potential function $\phi(x, y, t)$ that satisfies Laplace ' equation (2.15) and the two boundary conditions (3.7) and (3.10). Although it is very easy to guess what form the function should take for sinusoidal waves in the x direction , we shall find it instructive to proceed by the more formal method of separation of variables. We accordingly assume that a suitable solution of (2.26) , satisfying the two boundary conditions, has the form

$$\phi(x, y, t) = X(x) \cdot Y(y) \cdot T(t). \qquad (3.11)$$

Substitution of this trial solution into (2.26) gives no information about the time function $T(t)$, other than that it is satisfactory to have the time dependence of ϕ as a separate factored-out function $T(t)$. For the spatial functions, we find that

$$\frac{d^2 X}{dx^2} + \kappa^2 X = 0, \qquad (3.12)$$

$$\frac{d^2 Y}{dy^2} - \kappa^2 Y = 0, \qquad (3.13)$$

where the separation constant κ^2 has been given the sign that makes $X(x)$ a periodic function of x. General solutions of the separated equations are

$$X(x) = Ae^{i\kappa x} + Be^{-i\kappa x} , \tag{3.14}$$

$$Y(y) = Ce^{\kappa y} + De^{-\kappa y} . \tag{3.15}$$

We could have written these two solutions using trigonometric and hyperbolic functions , respectively.

We next need to introduce the boundary conditions at the bottom and at the top of the water. At the bottom , for all values of x and t, We have

$$v_y = -\frac{\partial \phi}{\partial y} = -XT\frac{dY}{dy} = 0 . \tag{3.16}$$

This condition requires that $C = D$, so that the Y function becomes

$$Y(y) = 2C\cosh \kappa y . \tag{3.17}$$

For simplicity we take $B = 0$, so that if $T(t)$ turns out to have the form $e^{-i\omega t}$, the solution we are constructing will represent sinusoidal waves traveling in the positive x direction.

We have established that the velocity potential has the form

$$\phi = A\cosh \kappa y \, e^{i\kappa x} T(t) \tag{3.18}$$

where A is an arbitrary constant. As a last step, let us substitute (3.18) in (3.10) , which is the remaining boundary condition at $y = h$, to obtain the equation for $T(t)$

$$\frac{d^2T}{dt^2} + (g\kappa \tanh \kappa h)T = 0 . \tag{3.19}$$

Hence the method of separation of variables has led us to a simple harmonic time dependence with the angular frequency

$$\omega = (g\kappa \tanh \kappa h)^{1/2} . \tag{3.20}$$

If we choose for T the solution $e^{-i\omega t}$, then

$$\phi = A\cosh \kappa y\, e^{i(\kappa x-\omega t)} \qquad (3.21)$$

is the velocity potential for a simple harmonic surface wave traveling in the positive x direction with a wave velocity

$$c = \frac{\omega}{\kappa} = \left(\frac{g}{\kappa}\tanh \kappa h\right)^{1/2}. \qquad (3.22)$$

As suggested by the notation, the separation constant κ is the wave number. The dependence of the wave velocity on wave number indicates that dispersion exists, so that a distinction must be made between phase and group velocity. A plot of (3.22) showing c as a function of wavelength for several depths h is given in Figure 3.4

For deep water, say when $h \geq \lambda/2$, $\tanh \kappa h \geq \tanh \pi = 0.996$, so that the expression for the wave velocity (3.22) becomes, very closely,

$$c = \left(\frac{g}{\kappa}\right)^{1/2} = \left(\frac{\lambda g}{2\pi}\right)^{1/2} \quad ; \quad (\lambda < h) \qquad (3.23)$$

Waves commonly seen on the ocean and on most lakes are of this type. In contrast , when the wavelength is much greater than the depth, i.e., when $\kappa h << 1$, $\tanh \kappa h \approx \kappa h$, and (3.22) now becomes, very closely ,

$$c = \left(\frac{g}{\kappa}\right)^{1/2} (h\kappa)^{1/2} = (gh)^{1/2} \quad ; \quad (\lambda >> h). \qquad (3.24)$$

Waves of this type therefore travel with a speed that varies with the square root of the depth but without dispersion.

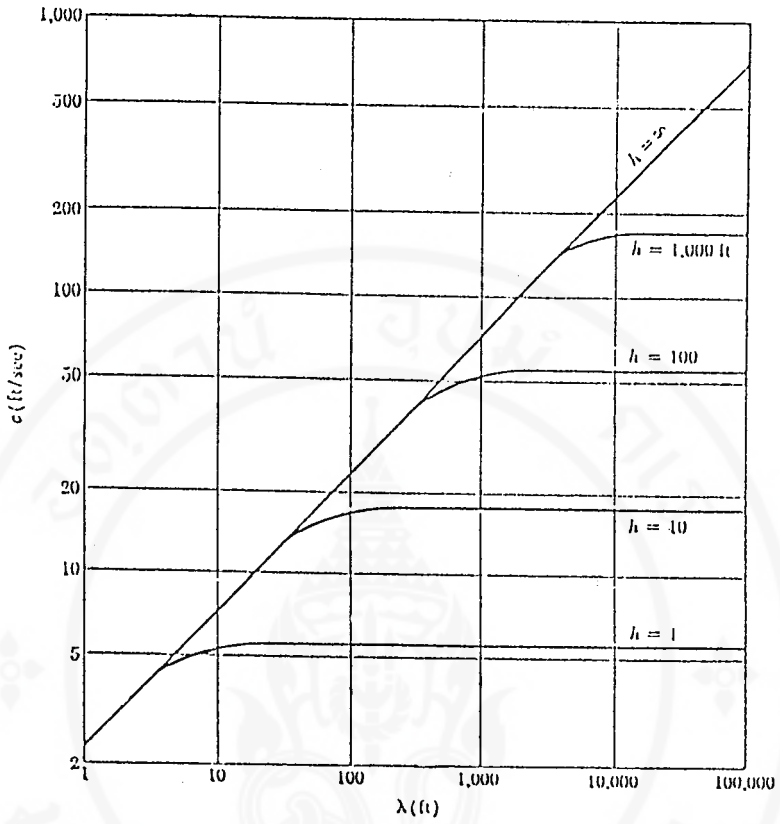

Figure 3.4 Velocity of water waves as a function of wavelength and depth.

Let us now obtain expressions for the displacement components in a wave having the velocity potential (3.21), which has the real part (assume that A is real)

$$\phi = A\cosh \kappa y \cos(\kappa x - \omega t). \tag{3.25}$$

The displacement velocity of the water, from (2.26) and (3.25) , has the components

$$\begin{aligned} v_x &= \frac{\partial \xi}{\partial t} = A\kappa \cosh \kappa y \sin(\kappa x - \omega t). \\ v_y &= \frac{\partial \eta}{\partial t} = -A\kappa \sinh \kappa y \cos(\kappa x - \omega t). \end{aligned} \tag{3.26}$$

Integrating with respect to time and setting $\eta_m \equiv (A\kappa/\omega)\sinh \kappa h$ for the vertical amplitude of the wave at the surface gives

$$\begin{aligned} \xi &= \eta_m \frac{\cosh \kappa y}{\sinh \kappa h} \cos(\kappa x - \omega t), \\ \eta &= \eta_m \frac{\sinh \kappa y}{\sinh \kappa h} \sin(\kappa x - \omega t). \end{aligned} \tag{3.27}$$

These are the parametric equations of the ellipse

$$\frac{\xi^2}{a^2} + \frac{\eta^2}{b^2} = 1 \tag{3.28}$$

having the major and minor semiaxes

$$\begin{aligned} a &= \eta_m \frac{\cosh \kappa y}{\sinh \kappa h}, \\ b &= \eta_m \frac{\sinh \kappa y}{\sinh \kappa h}. \end{aligned} \tag{3.29}$$

The axes of the ellipse diminish with depth, the minor axis b vanishing at the bottom. When the depth of water is of the order of one wavelength or greater, $e^{-\kappa h}$ is very small (so that $a \approx b$) and the ellipses become very nearly circles with radii that decrease exponentially with depth. These waves have the velocity (3.23).

When the depth is much less than a wavelength , i.e. , when $\kappa h << 1$, then $\cosh \kappa y \approx 1$, $\sinh \kappa y \approx \kappa y$, and

$$\begin{aligned} a &\approx \frac{\eta_m}{\kappa h}, \\ b &\approx \eta_m \frac{y}{h}. \end{aligned} \tag{3.30}$$

For this case of shallow water, the horizontal motion of the water due to a wave is the same at all depths, with the vertical motion decreasing linearly with amplitude to the bottom where it vanishes. A wave of this type, whose velocity is given by (3.24) , is usually termed a *tidal wave*.

If we compare the equations for the displacement velocity (3.26) with those for the particle displacement (3.27), we see that the water making up a crest of the wave is moving in the direction in which the wave is traveling, whereas the water in a trough is moving in the backward direction. Although both the ξ and η displacements depend sinusoidally on $\kappa x - \omega t$ the first with a cosine, the second with a sine factor, the actual profile of the water surface differs slightly from a sine wave. At the top of a crest, where $\eta = \eta_m$, ξ is zero; in the half-wavelength behind this point , ξ is positive , whereas in the half-wavelength in front of it, ξ is negative. Evidently the crests are somewhat narrower than those of a pure sine wave, whereas the troughs are correspondingly wider. For waves of finite amplitude, the sort of distortion just described is considerably greater than that predicted by the present linearized theory.

2. Lagrange Multipliers Method

From equations (2.2) - (2.4) we have the Lagrangian L ,

$$L = \sum_{t=1}^{n}\left[h_{obs}(t) - (a_0 + a_1 \sin t + a_2 \cos t)\right]^2 + \sum_{t=1}^{n}\lambda_t R_t \ . \qquad (3.31)$$

Where the sum on the second term is used to indicate that there are as many Lagrange multipliers as there are constraint equations and integrals over space and time as well. The constraint equations are due to the basis hydrodynamics , the displacement velocity of the water at any position and time (3.26). Integrating with respect to time and set $\eta_m \equiv (A\kappa/\omega)\sinh \kappa h$ for the vertical amplitude of the wave at the surface gives (3.27) and when the depth is much less than a wavelength, i.e., when $\kappa h << 1$, then $\cosh \kappa y \approx 1, \sinh \kappa y \approx \kappa y$. We have

$$\begin{aligned} \xi &= \frac{\eta_m}{\kappa h}\cos(\kappa x - \omega t) , \\ \eta &= \eta_m \frac{y}{h}\sin(\kappa x - \omega t). \end{aligned} \tag{3.32}$$

Input initial condition to equations (3.32) are

$$\begin{aligned} \xi - f(a_0, a_1, a_2) &= 0 , \\ \eta - g(a_0, a_1, a_2) &= 0. \end{aligned} \tag{3.33}$$

Thus the Lagrangian L, from equation (3.31) takes on the form

$$L = \sum_{t=1}^{n}\left[\left[h_{obs}(t) - (a_0 + a_1 \sin t + a_2 \cos t)\right]^2 + \lambda_{1t}\left(\xi - f(a_0, a_1, a_2)\right) + \lambda_{2t}\left(\eta - g(a_0, a_1, a_2)\right)\right]. \tag{3.34}$$

Take the derivatives of L with respect to parameters

$$\begin{aligned} \frac{\partial L}{\partial a_i} &= 0 \quad ; \quad i = 0, 1, 2 \\ \frac{\partial L}{\partial \lambda_{1t}} &= 0 \quad ; \quad t = 1, 2, 3 \\ \frac{\partial L}{\partial \lambda_{2t}} &= 0 \quad ; \quad t = 1, 2, 3 \ . \end{aligned} \tag{3.35}$$

We obtain the system of equations (3.35) containing 9 equations and 9 unknowns. So solving the system of equations , by a computer program , we write

$$h(t) = a_0' + a_1' \sin t + a_2' \cos t . \tag{3.36}$$

CHAPTER IV

RESULTS AND DISCUSSION

In this chapter, we apply the methods developed in chapter III to the analysis of the mixed tide data taken at Hua-Hin , Pak Nam Tachin and Ko Sichang. These sets of data are analyzed using the data assimilation techniques and the least square best fit techniques. The prediction of the two methods are compared by the sum square error (SSE.) .

We begin by noting that accurate data are needed for good predictions of the height of the tide. Since the errors in the observation data may arise from break down of the instrument or inaccurate observations, we have eliminated obvious data errors and replaced them by these extrapolated values taken from nearly values. To check whether a data point is the result of missed observation, we have taken the mean value of the data from data of the previous 24 hours and used equations (3.1) and (3.2) to interpolate the value.

The raw data points at the Hua-Hin and Pak Nam Tachin stations exhibit several points outside the interval $[0,5]$. The data for the Ko Sichang station does not contain any points outside the interval $[0,5]$. In table 4.1, we list the number of error points in the data set for the three stations in 1996. Figure 4.1 – Figure 4.13 shows graphs for the actual (error containing) data and the equivalent interpolated values at each station.

Table 4.1 Example number of error data monthly each station in 1996

Month	Number of error data		
	Hua-Hin	**Pak Nam Tachin**	**Ko Sichang**
January	17	36	0
February	22	1	0
March	0	0	0
April	16	0	0
May	0	0	0
June	0	0	0
July	0	29	0
August	0	0	0
September	26	0	0
October	0	0	0
November	16	23	0
December	78	12	0
Total	175	101	0

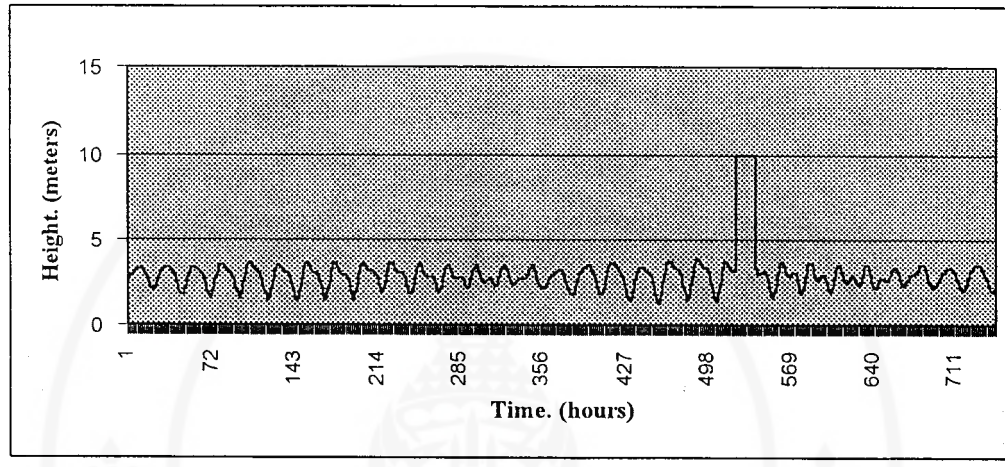

Figure 4.1 (a) Graph of error data observation Hua-Hin station on January

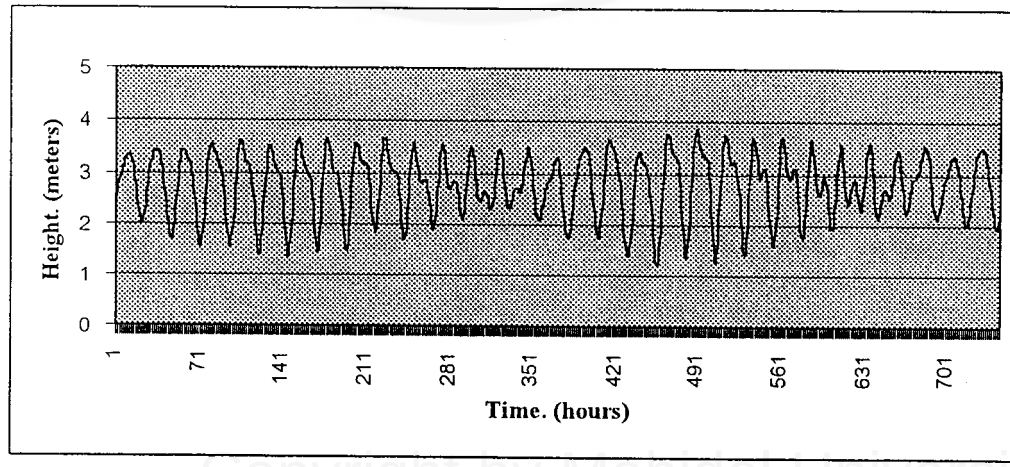

Figure 4.1 (b) Graph of data interpolation Hua-Hin station on January

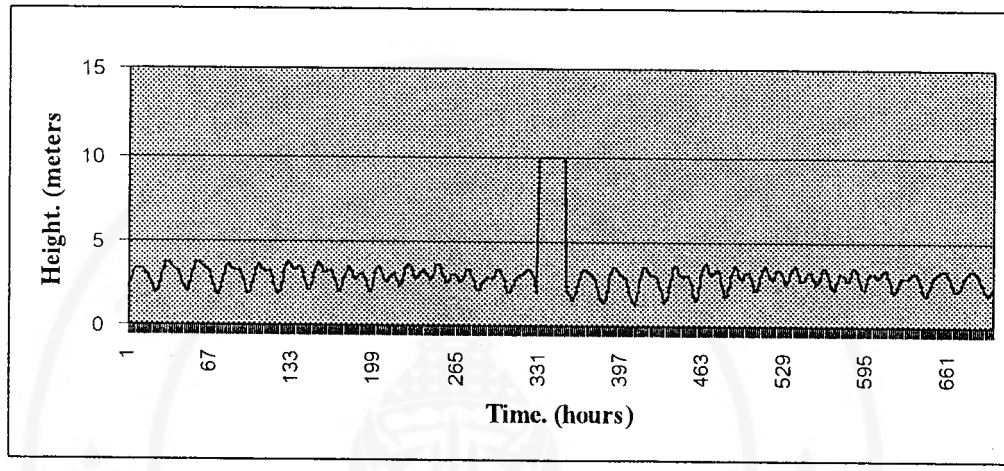

Figure 4.2 (a) Graph of error data observation Hua-Hin station on February

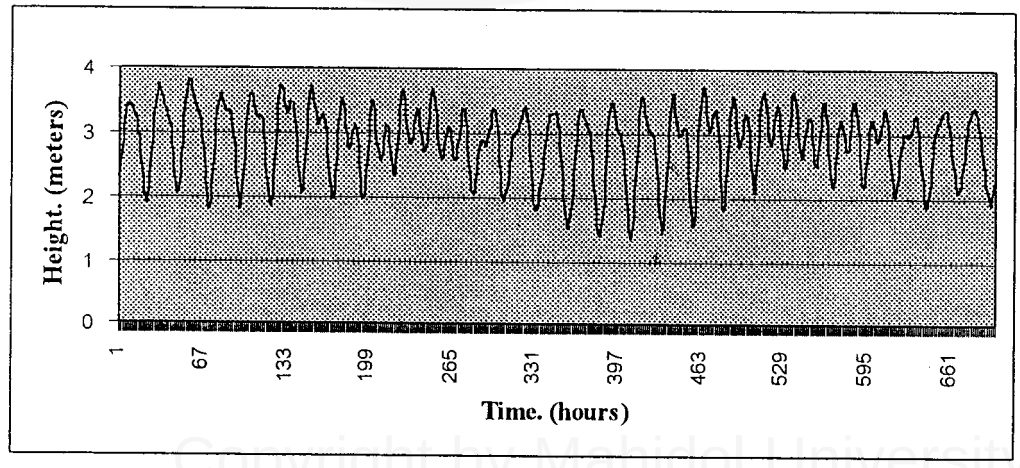

Figure 4.2 (b) Graph of data interpolation Hua-Hin station on February

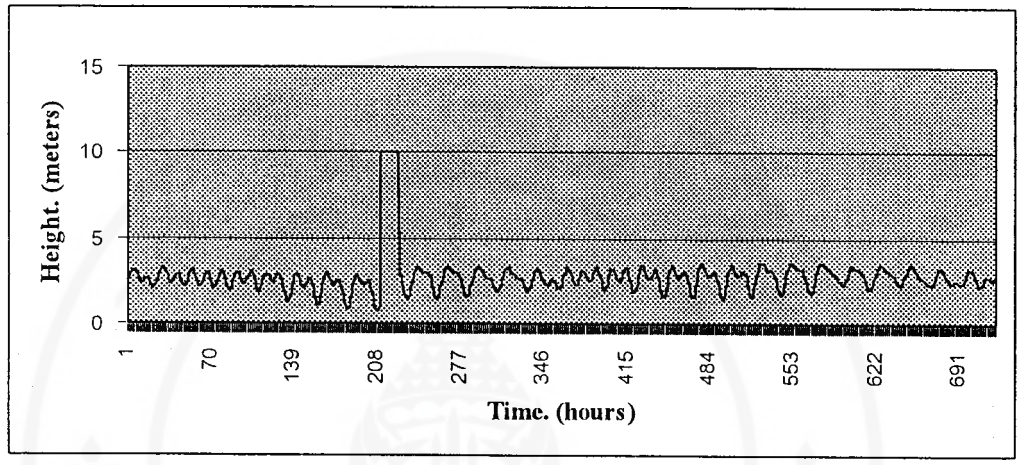

Figure 4.3 (a) Graph of error data observation Hua-Hin station on April

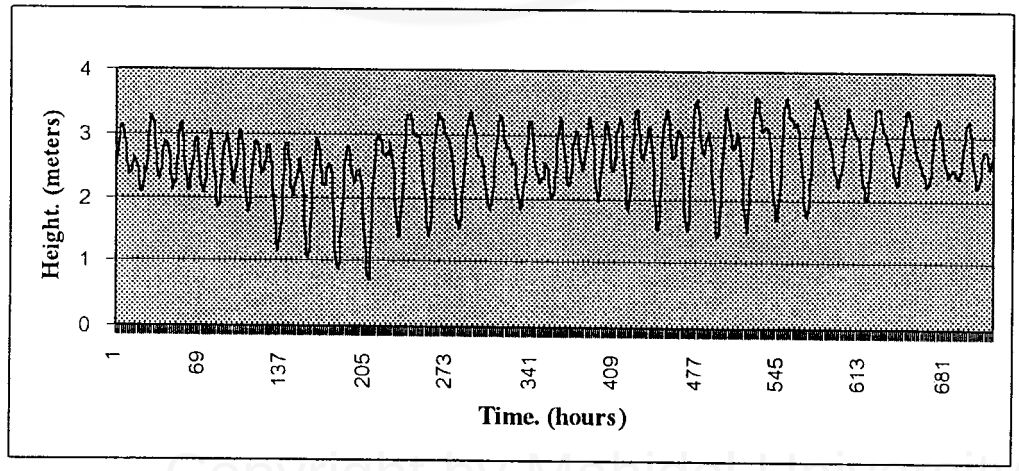

Figure 4.3 (b) Graph of data interpolation Hua-Hin station on April

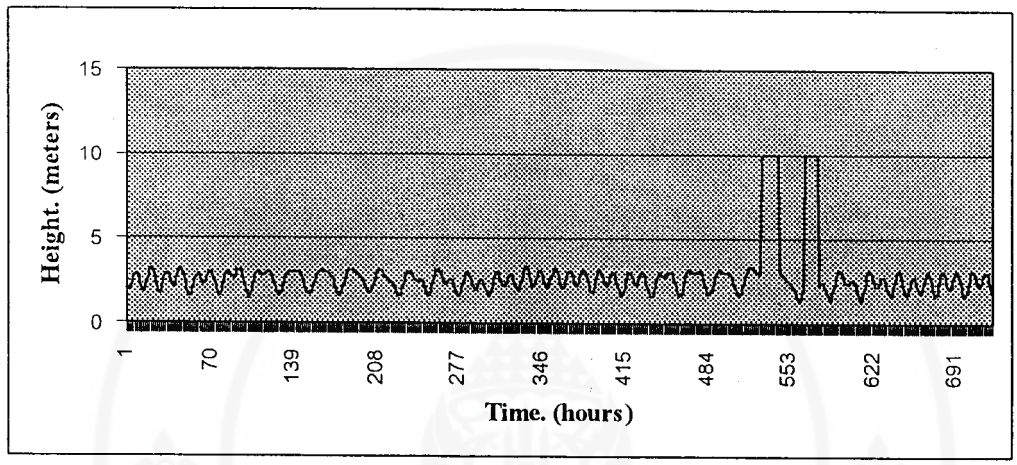

Figure 4.4 (a) Graph of error data observation Hua-Hin station on September

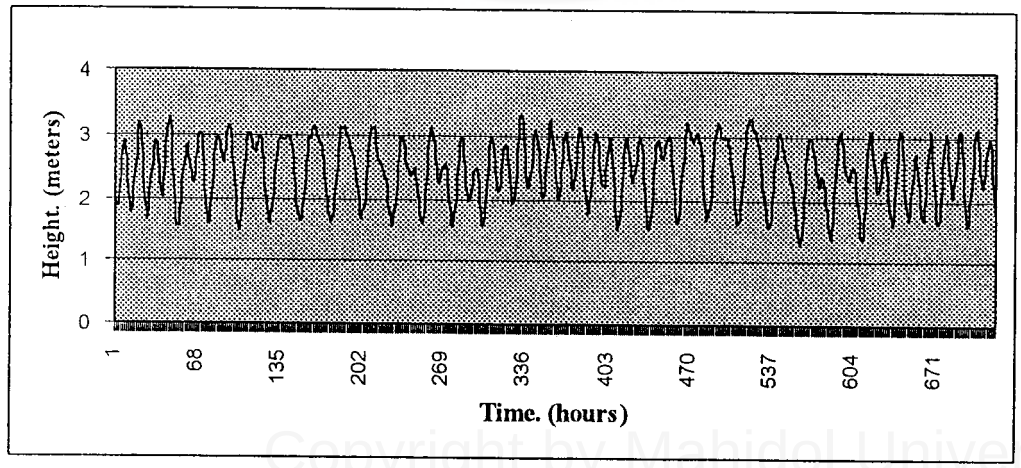

Figure 4.4 (b) Graph of data interpolation Hua-Hin station on September

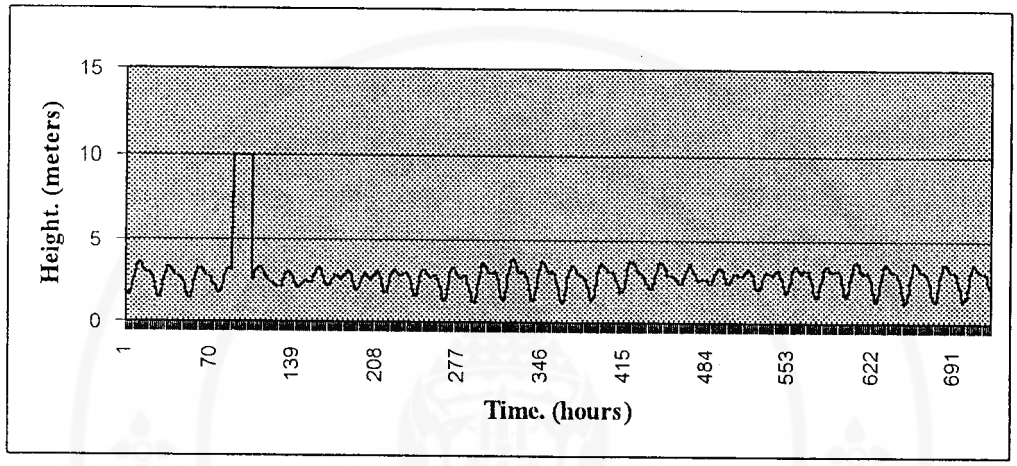

Figure 4.5 (a) Graph of error data observation Hua-Hin station on November

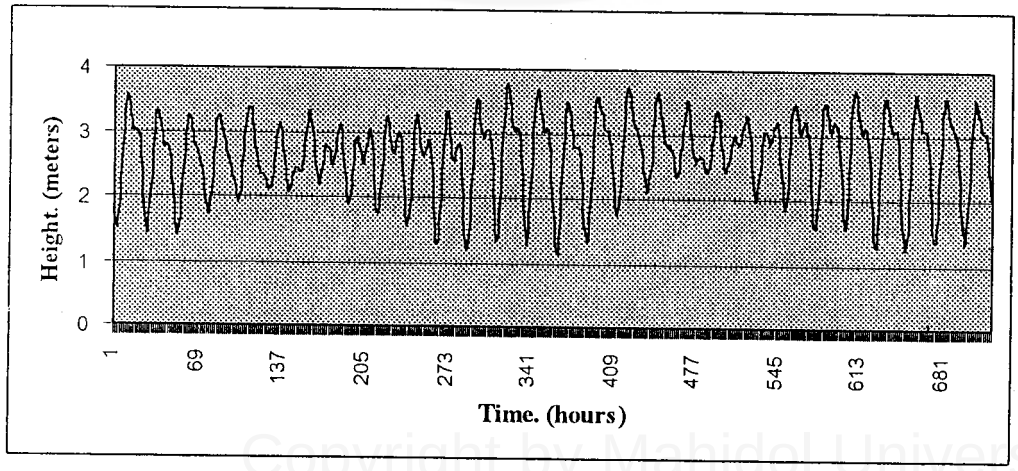

Figure 4.5 (b) Graph of data interpolation Hua-Hin station on November

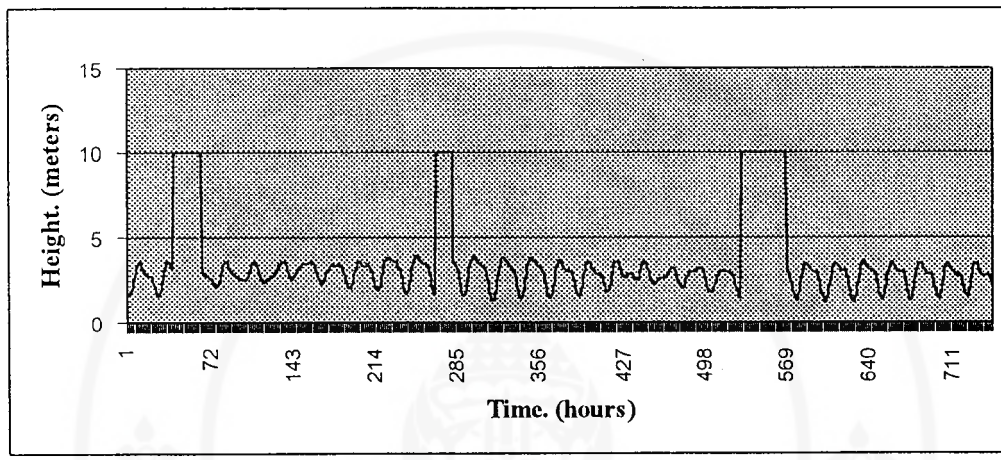

Figure 4.6 (a) Graph of error data observation Hua-Hin station on December

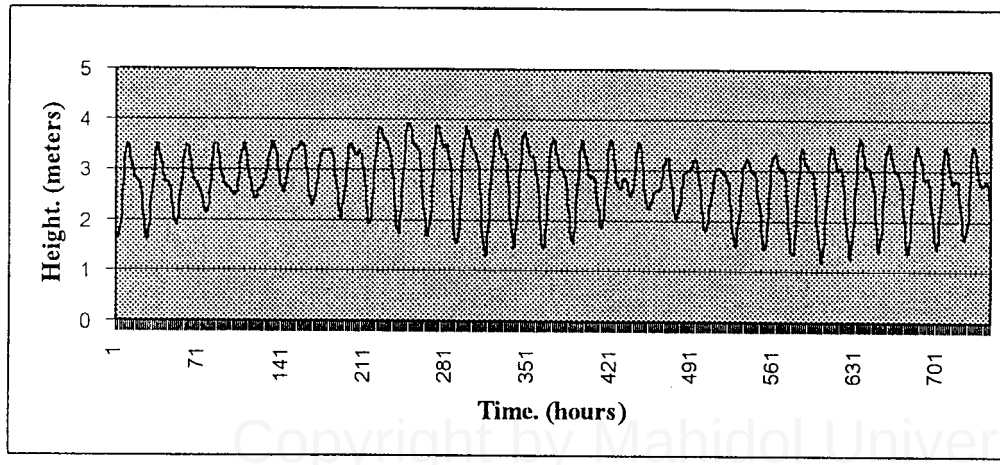

Figure 4.6 (b) Graph of data interpolation Hua-Hin station on December

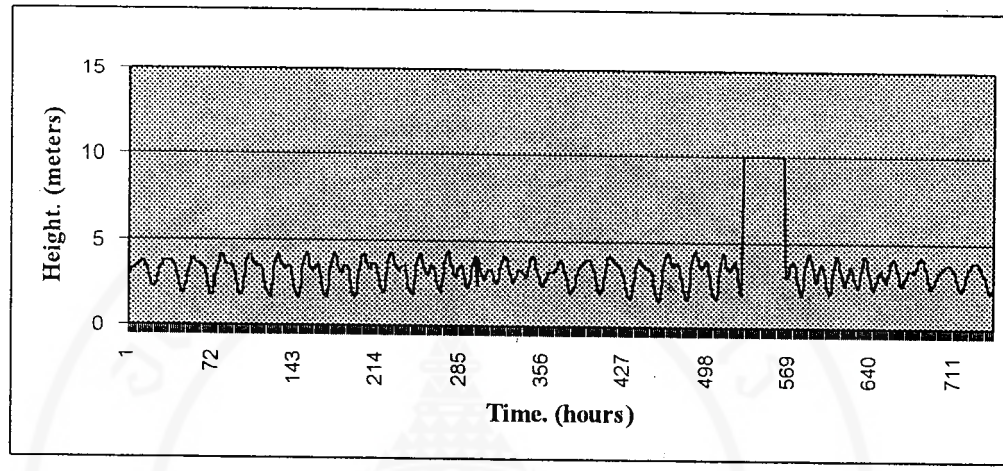

Figure 4.7 (a) Graph of error data observation

Pak Nam Tachin station on January

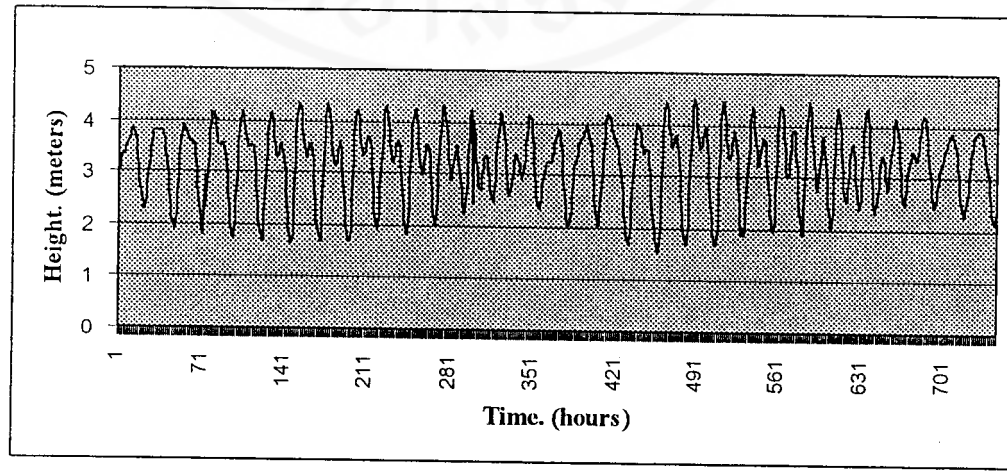

Figure 4.7 (b) Graph of data interpolation

Pak Nam Tachin station on January

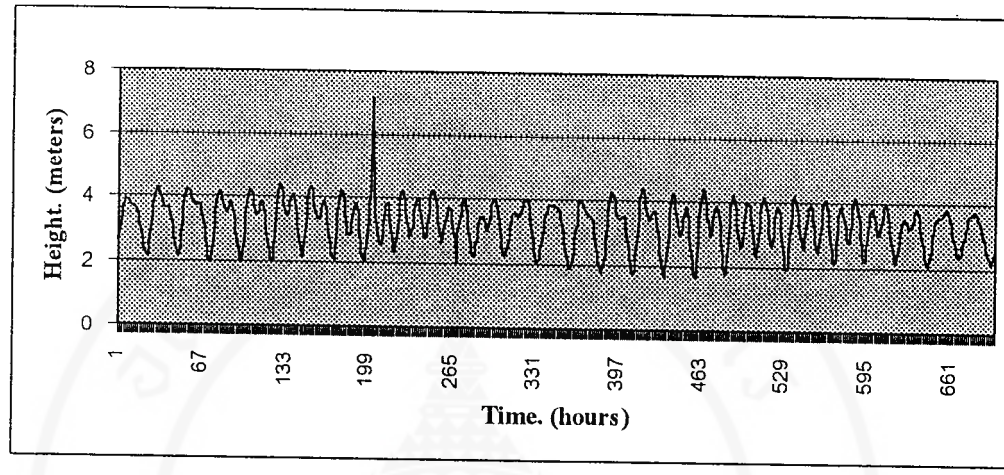

Figure 4.8 (a) Graph of error data observation

Pak Nam Tachin station on February

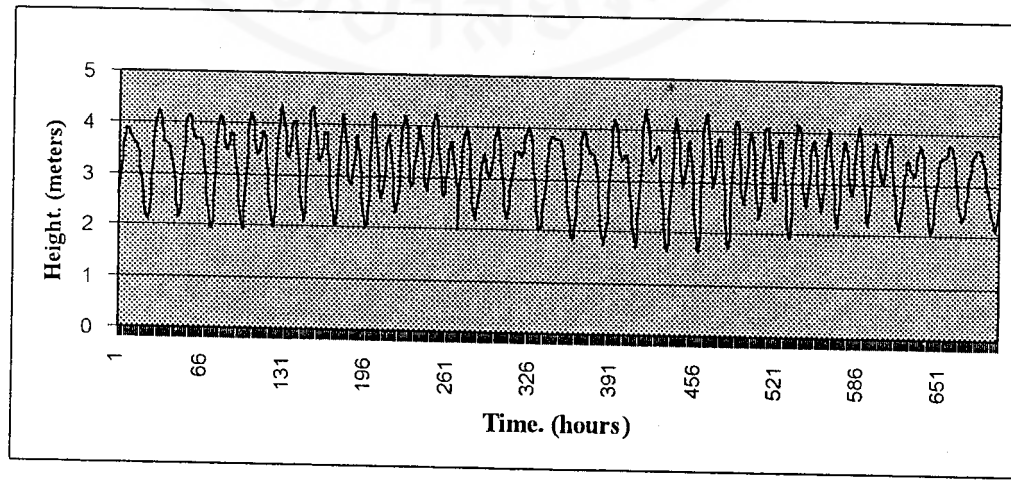

Figure 4.8 (b) Graph of data interpolation

Pak Nam Tachin station on February

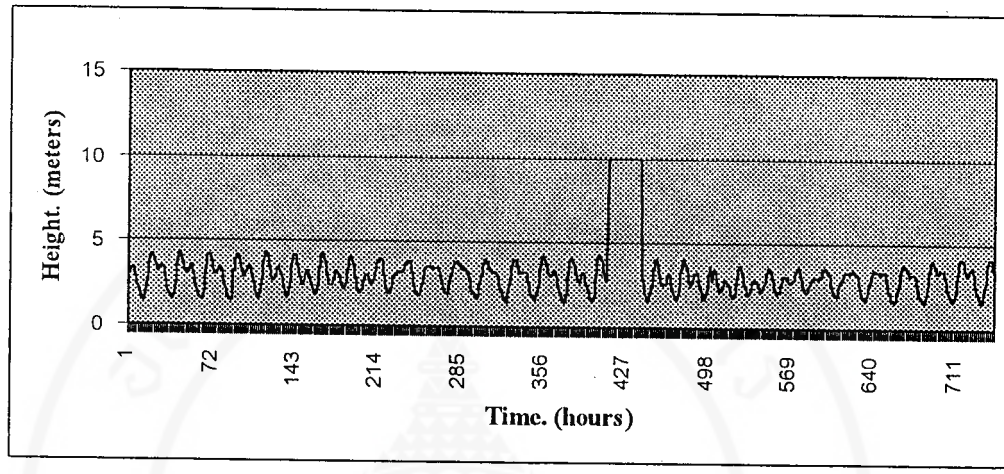

Figure 4.9 (a) Graph of error data observation

Pak Nam Tachin station on July

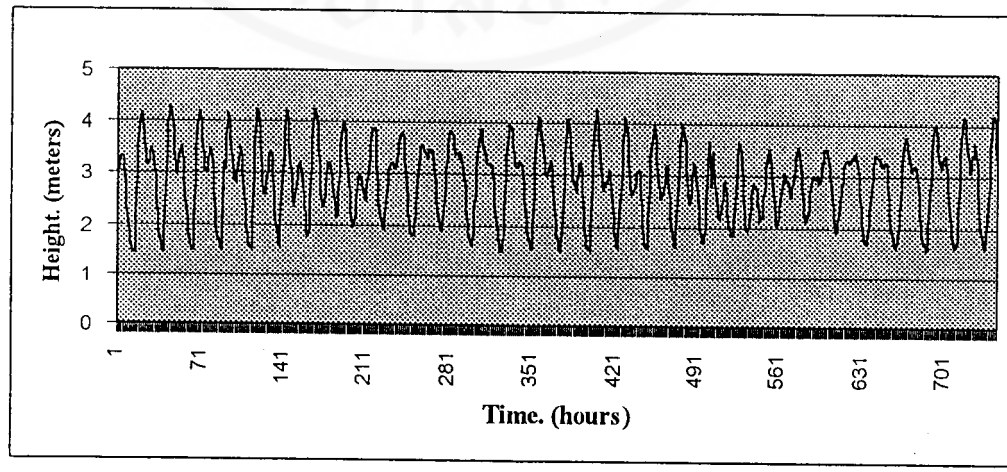

Figure 4.9 (b) Graph of data interpolation

Pak Nam Tachin station on July

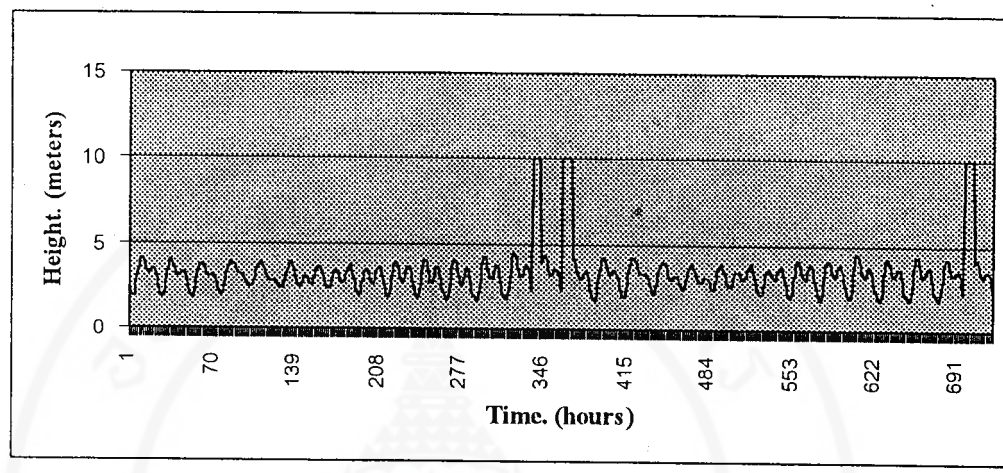

Figure 4.10 (a) Graph of error data observation

Pak Nam Tachin station on November

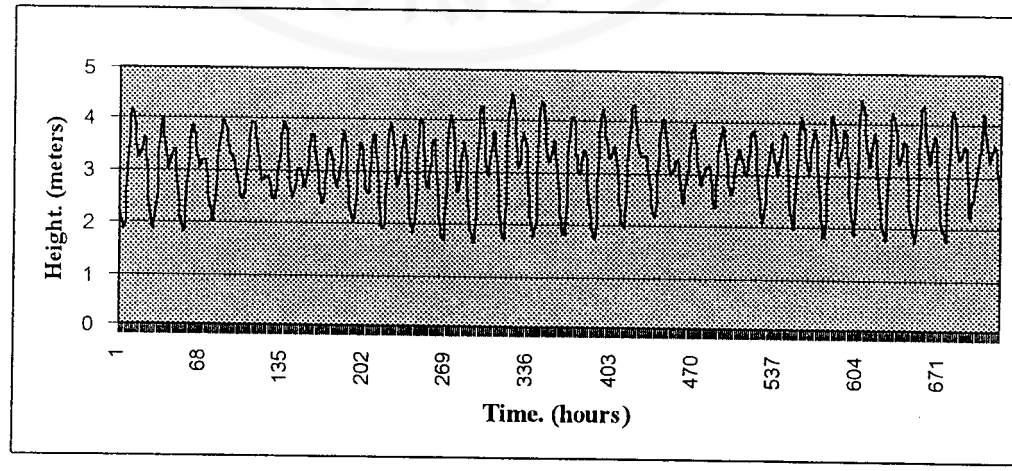

Figure 4.10 (b) Graph of data interpolation

Pak Nam Tachin station on November

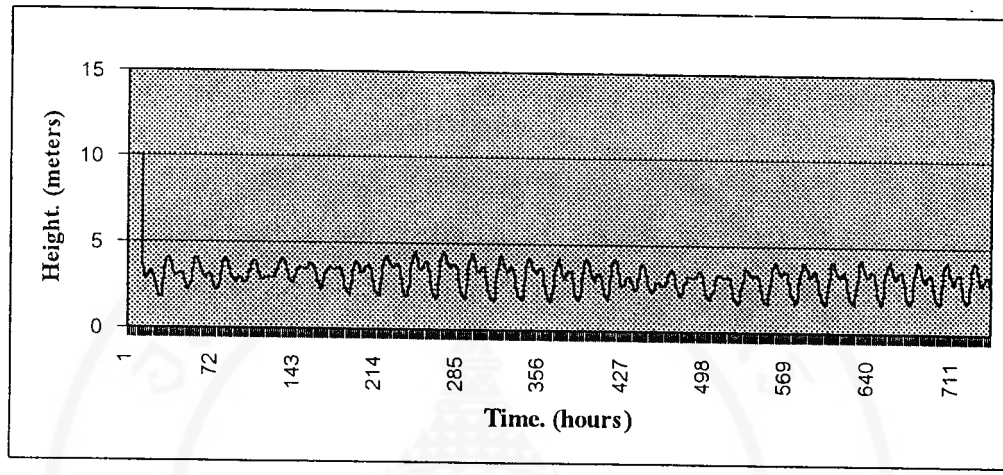

Figure 4.11 (a) Graph of error data observation

Pak Nam Tachin station on December

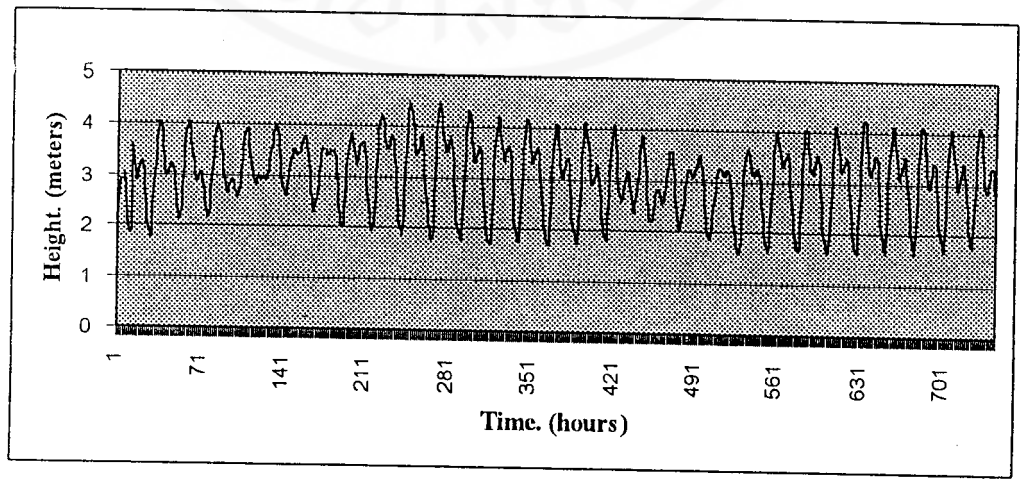

Figure 4.11 (b) Graph of data interpolation

Pak Nam Tachin station on December

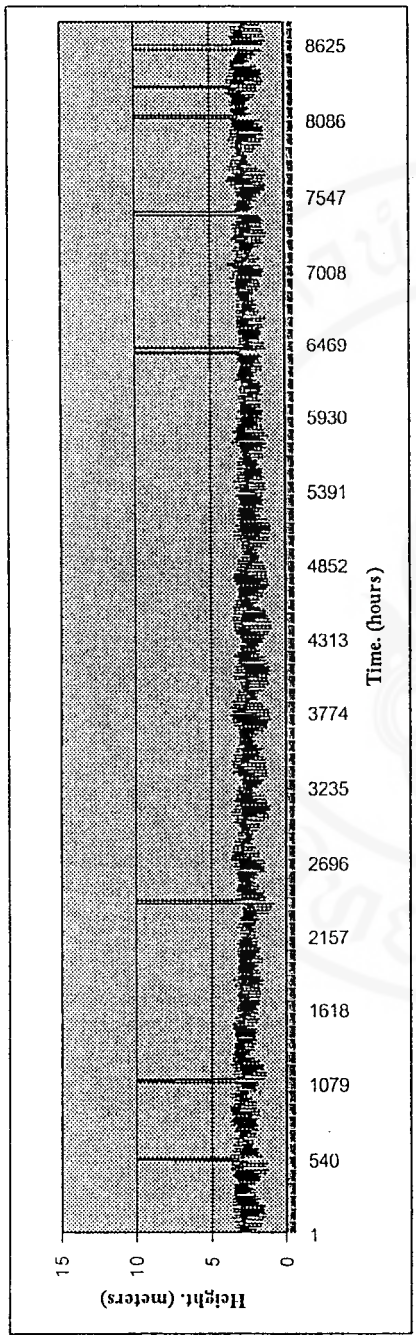

Figure 4.12 (a) Graph of error data observation Hua-Hin station in 1996

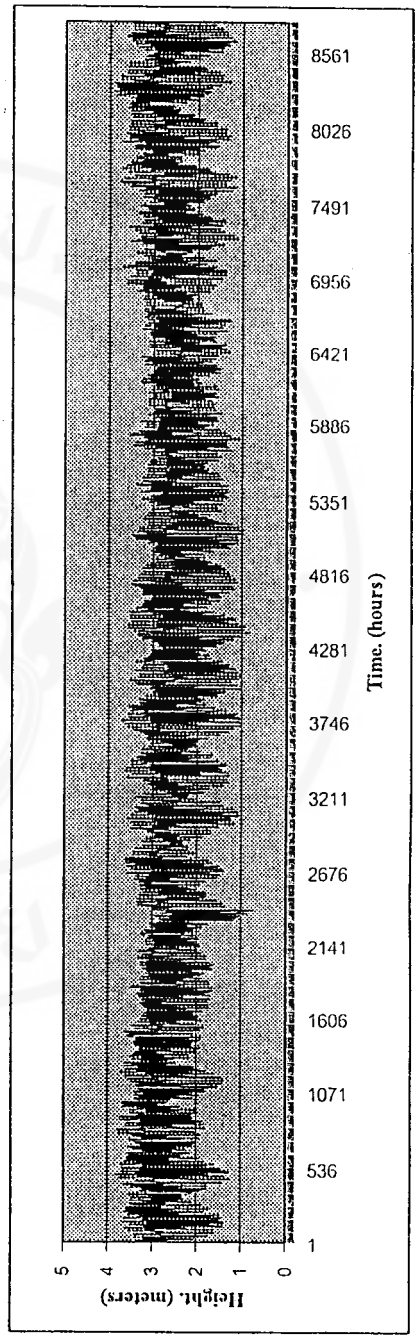

Figure 4.12 (b) Graph of data interpolation Hua-Hin station in 1996

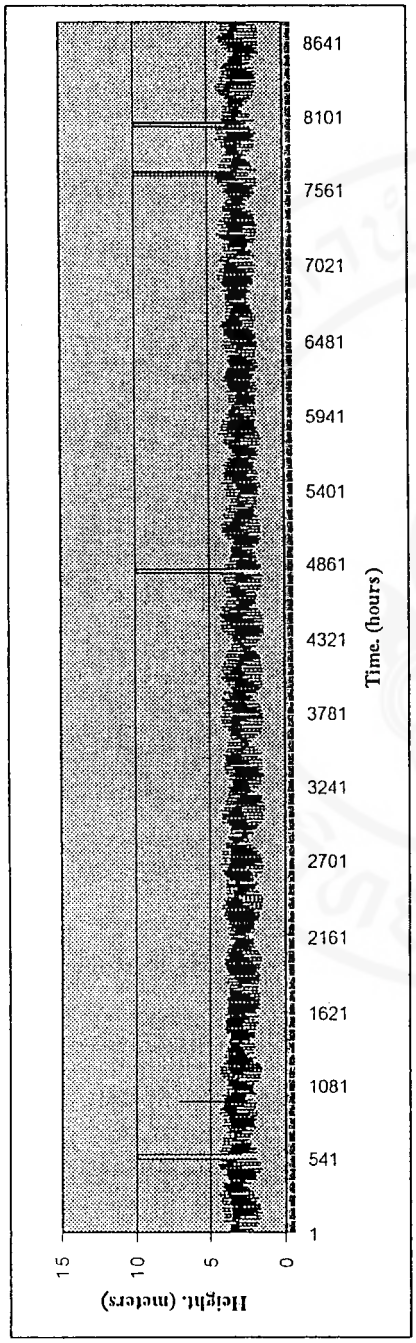

Figure 4.13 (a) Graph of error data observation Pak Nam Tachin station in 1996

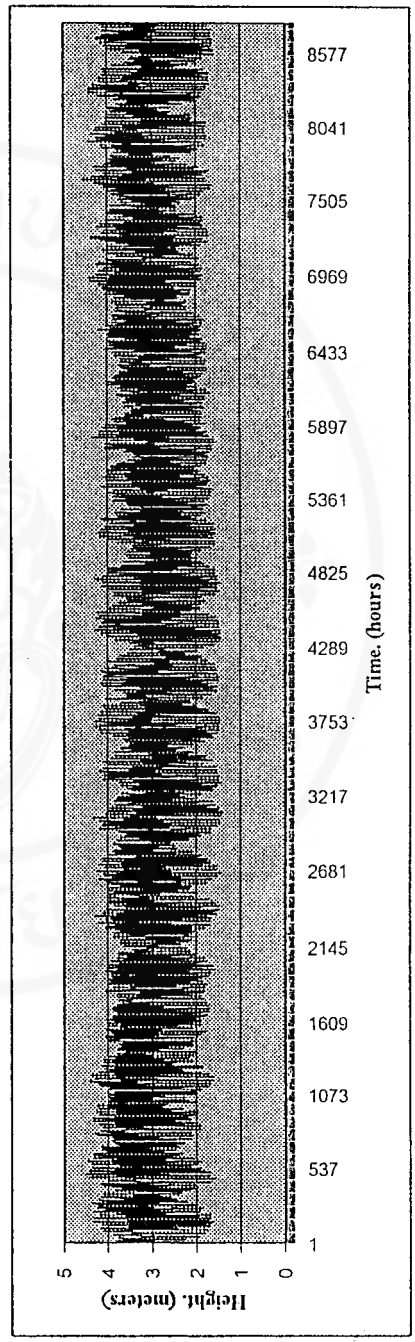

Figure 4.13 (b) Graph of data interpolation Pak Nam Tachin station in 1996

Results of Model from Least Square Best Fits.

Using the interpolated data of each station , we calculate the parameters a_0 , a_1 and a_2 in the least square best fit model. There are obtained by solving the following equation (3.6)

$$\begin{bmatrix} n & \sum_{t=1}^{n}\sin t & \sum_{t=1}^{n}\cos t \\ \sum_{t=1}^{n}\sin t & \sum_{t=1}^{n}\sin^2 t & \sum_{t=1}^{n}\sin t\cos t \\ \sum_{t=1}^{n}\cos t & \sum_{t=1}^{n}\sin t\cos t & \sum_{t=1}^{n}\cos^2 t \end{bmatrix} \begin{bmatrix} a_0 \\ a_1 \\ a_2 \end{bmatrix} = \begin{bmatrix} \sum_{t=1}^{n}h(t) \\ \sum_{t=1}^{n}h(t)\sin t \\ \sum_{t=1}^{n}h(t)\cos t \end{bmatrix}$$

Table 4.2 list the values of parameters a_0 , a_1 and a_2 from least square best fits each station in 1996. Table 4.3 – Table 4.5 list value of parameters a_0 , a_1 and a_2 by least square best fits each monthly station in 1996.

Figure 4.14 (a) - (c) show example of graph height of tide prediction by least square best fit each station.

Table 4.2 Value parameters from Least Square Best fit in 1996.

Station	Number of data	a_0	a_1	a_2
Hua-Hin	8784	2.58650	0.00050	-0.00060
Pak Nam Tachin	8784	2.98690	0.00060	-0.00090
Ko Sichang	8784	2.52190	-0.00300	-0.00010

Table 4.3 Value parameters of Hua-Hin station by Least Square Best fit for monthly in 1996

Month	**Number of data**	a_0	a_1	a_2
January	744	2.7506	-0.0037	-0.0014
February	696	2.8421	-0.0037	0.0021
March	744	2.6515	-0.0036	-0.0009
April	720	2.5722	-0.0056	-0.0009
May	744	2.5357	0.0000	-0.0016
June	720	2.4411	0.0001	-0.0024
July	744	2.4243	0.0048	0.0023
August	744	2.3897	-0.0001	-0.0001
September	720	2.4313	0.0025	0.0020
October	744	2.5905	-0.0020	0.0061
November	720	2.6586	-0.0027	0.0034
December	744	2.7596	-0.0035	0.0025

Table 4.4 Value parameters of Pak Nam Tachin station by Least Square Best fit for monthly in 1996

Month	**Number of data**	a_0	a_1	a_2
January	744	3.1858	0.0042	0.0110
February	696	3.2019	-0.0001	0.0020
March	744	3.0006	0.0101	-0.0032
April	720	3.0011	-0.0034	0.0053
May	744	2.8595	0.0103	0.0054
June	720	2.8480	0.0108	-0.0140
July	744	2.8423	-0.0012	-0.0217
August	744	2.8516	-0.0186	0.0168
September	720	2.8704	0.0130	0.0256
October	744	3.0603	0.0108	0.0099
November	720	3.0997	0.0077	0.0049
December	744	3.0288	-0.0018	0.0092

Table 4.5 Value parameters of Ko Sichang station by Least Square Best fit for monthly in 1996

Month	Number of data	a_0	a_1	a_2
January	744	2.6101	-0.0014	0.0042
February	696	2.7618	0.0102	-0.0027
March	744	2.5884	-0.0043	-0.0112
April	720	2.6330	-0.0191	0.0014
May	744	2.5682	0.0002	-0.0071
June	720	2.3817	0.0092	-0.0036
July	744	2.3520	0.0022	-0.0018
August	744	2.3866	0.0031	0.0017
September	720	2.4238	-0.0046	0.0103
October	744	2.5401	-0.0052	0.0069
November	720	2.5552	-0.0095	0.0086
December	744	2.5596	-0.0040	0.0027

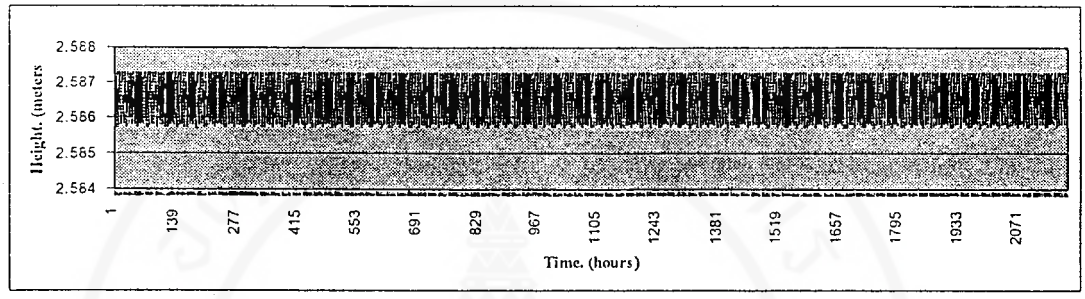

Figure 4.14 (a) Graph of tide prediction Hua-Hin station by Least Square Best fit.

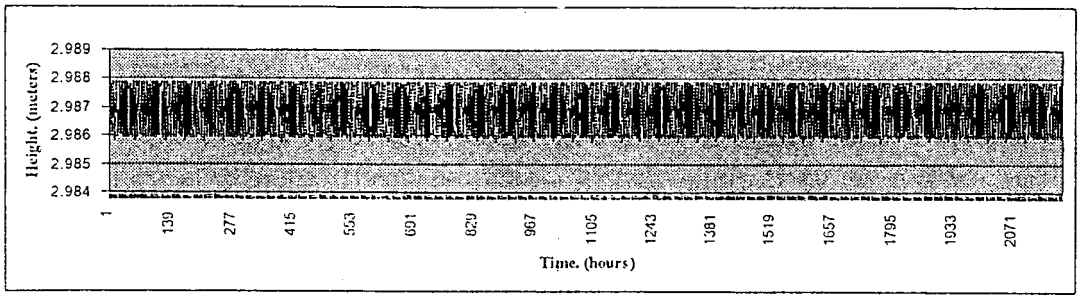

Figure 4.14 (b) Graph of tide prediction Pak Nam Tachin station by Least Square Best fit.

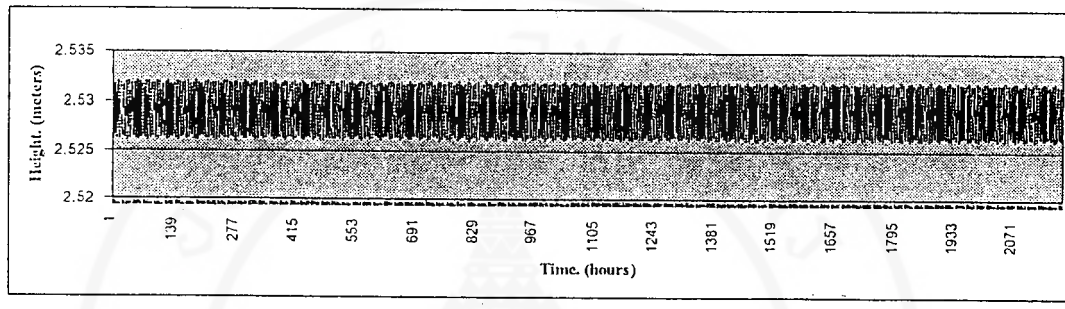

Figure 4.14 (c) Graph of tide prediction Ko Sichang station by Least Square Best fit.

From table 4.2 – table 4.5 we see value of parameter a_0 nearly value of mean sea level (2.5 meters) each station and value of absolute parameter a_1 and a_2 less than 0.01.

From figure 4.14 (a) – (c) we see that the height of tide are more than 2.5 meters and less than 3.0 meters.

Physical Constraint Equations

The constraint equations come from the basic equations of hydrodynamics of an idea fluid which consist of three categories :

1. *Kinematical equations* (2.5) - (2.11) , we have the linear velocity v can be derived from a scalar velocity potential ϕ , $v = -\nabla\phi$.

2. *The equation of continuity* (2.12) - (2.15) , which we consider in the case of an incompressible fluid , when the pressure change is small, the density ρ is a constant. The equation of continuity then becomes $\nabla \cdot v = 0$ and the velocity at any point in an incompressible liquid must satisfy *Laplace's equation* $\nabla \cdot \nabla\phi = 0$.

3. *The Bernoulli Equation* , when the fluid can be considered incompressible , from (2.25) and the two boundary conditions (3.7) and (3.9)

$$v_y = -\frac{\partial\phi}{\partial y} = 0 \qquad (y = 0) ,$$

$$v_y = -\frac{\partial\phi}{\partial y} = \frac{1}{g}\frac{\partial^2\phi}{\partial t^2} \qquad (y = h) .$$

From basic hydrodynamics and conditions we have the displacement velocity of the water at any position and time (3.26)

$$v_x = \frac{\partial\xi}{\partial t} = A\kappa \cosh \kappa y \sin(\kappa x - \omega t) ,$$

$$v_y = \frac{\partial\eta}{\partial t} = -A\kappa \sinh \kappa y \cos(\kappa x - \omega t) .$$

And when the depth is much less than a wavelength , we have (3.27)

$$\xi = \frac{\eta_m}{\kappa h}\cos(\kappa x - \omega t) \quad \text{and} \quad \eta = \eta_m \frac{y}{h}\sin(\kappa x - \omega t) .$$

where $\eta_m = (A\kappa/\omega)\sinh\kappa h$ for the vertical amplitude of the wave at the surface give (3.27).

Result of Model from Lagrange Multipliers Method.

From the Lagrangian L, (3.34) and equation of motion derived from physical constraint equations for each station, so we see same determine of tide at each station.

Figure 4.15 - Figure 4.17 properties of the output each station on 1996 by Lagrange multipliers method along with the value of parameters and value of sum square error (SSE.) .

Figure 4.18 - Figure 4.20 show graph height of tide prediction each station on 1996 by Lagrange multipliers method.

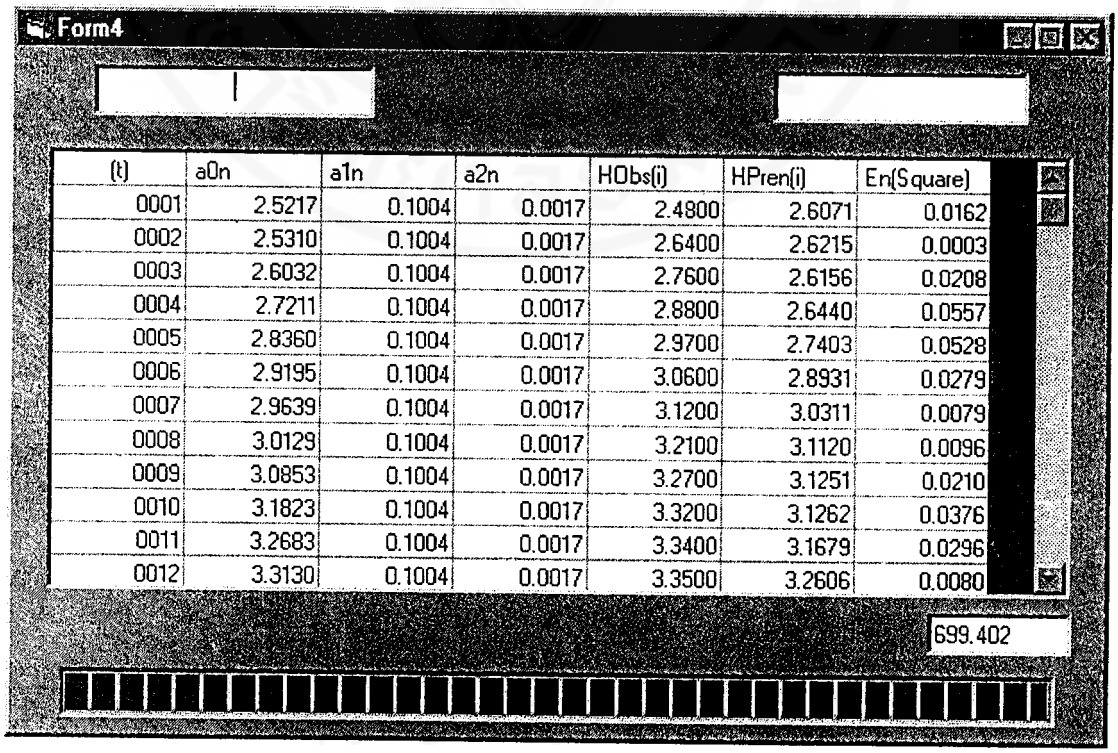

(t)	a0n	a1n	a2n	HObs(i)	HPren(i)	En(Square)
0001	2.5217	0.1004	0.0017	2.4800	2.6071	0.0162
0002	2.5310	0.1004	0.0017	2.6400	2.6215	0.0003
0003	2.6032	0.1004	0.0017	2.7600	2.6156	0.0208
0004	2.7211	0.1004	0.0017	2.8800	2.6440	0.0557
0005	2.8360	0.1004	0.0017	2.9700	2.7403	0.0528
0006	2.9195	0.1004	0.0017	3.0600	2.8931	0.0279
0007	2.9639	0.1004	0.0017	3.1200	3.0311	0.0079
0008	3.0129	0.1004	0.0017	3.2100	3.1120	0.0096
0009	3.0853	0.1004	0.0017	3.2700	3.1251	0.0210
0010	3.1823	0.1004	0.0017	3.3200	3.1262	0.0376
0011	3.2683	0.1004	0.0017	3.3400	3.1679	0.0296
0012	3.3130	0.1004	0.0017	3.3500	3.2606	0.0080

Figure 4.15 Output from program of Hau-Hin station in 1996 by Lagrange Multipliers Method

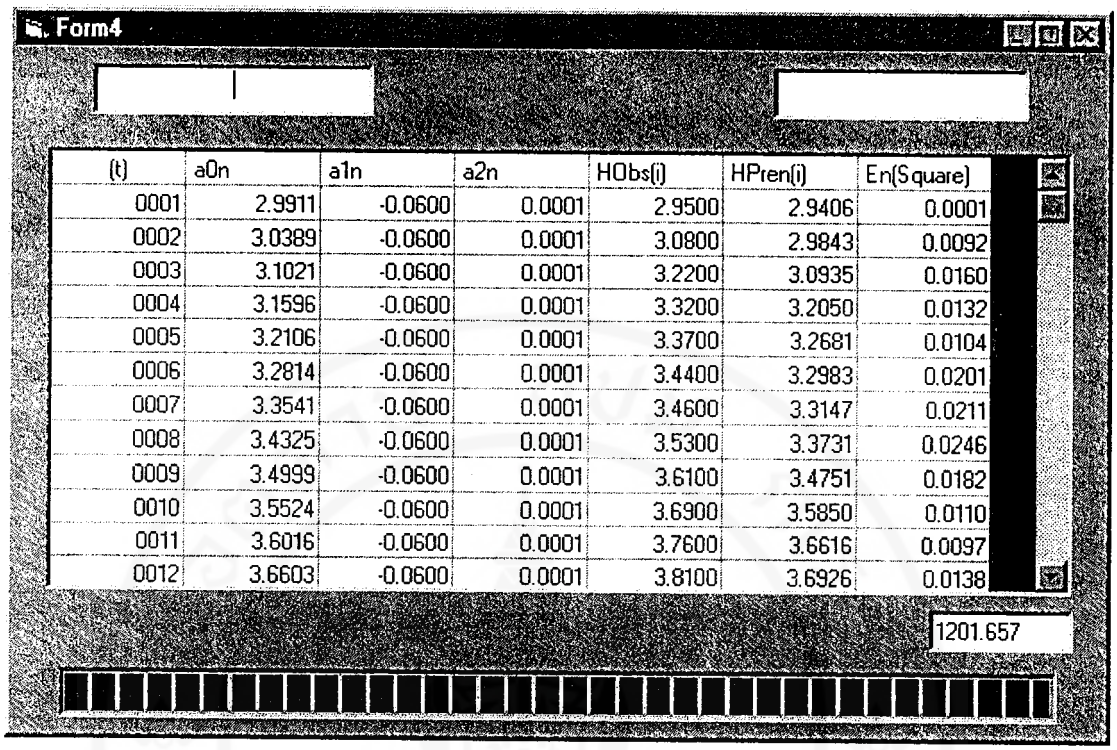

Figure 4.16 Output from program of Pak Nam Tachin station in 1996 by Lagrange Multipliers Method

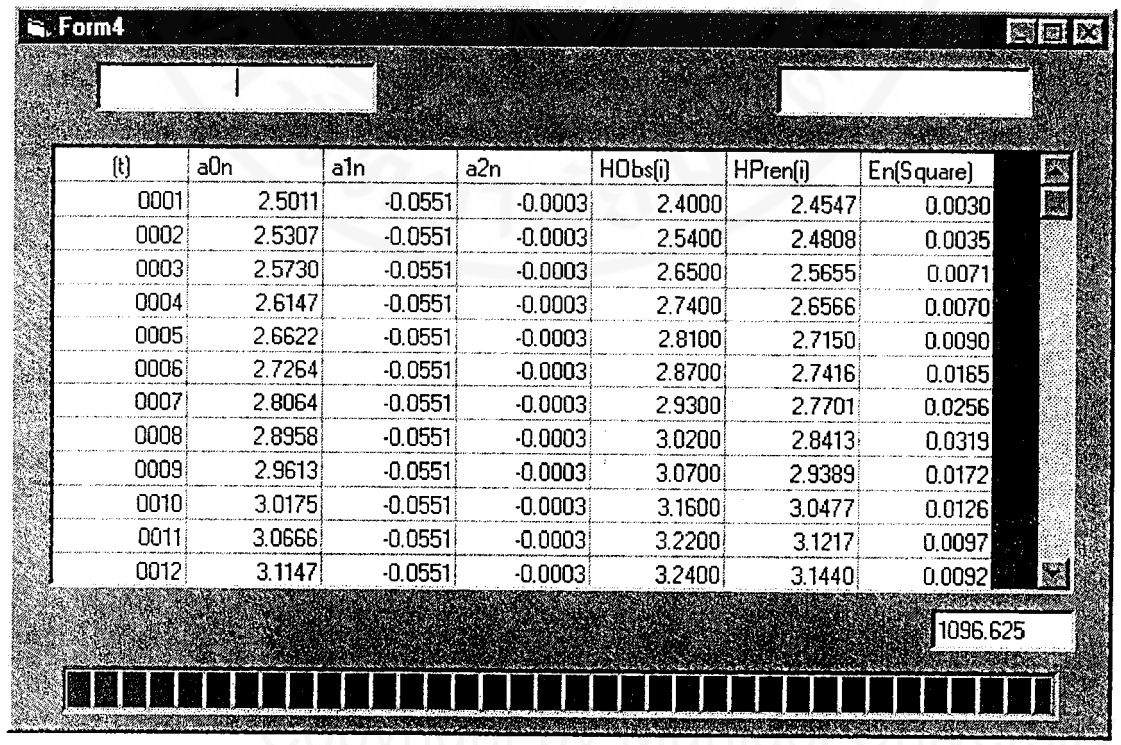

Figure 4.17 Output from program of Ko Sichang station in 1996 by Lagrange Multipliers Method

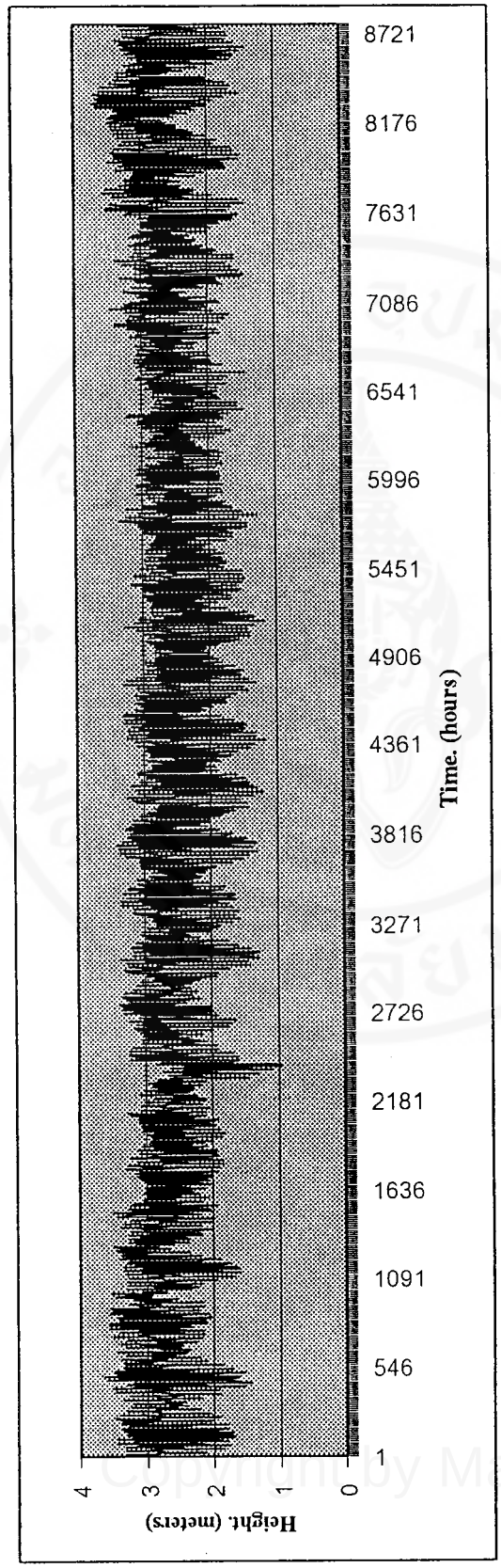

Figure 4.18 Graph of tide prediction Hua-Hin station by Lagrange multipliers method

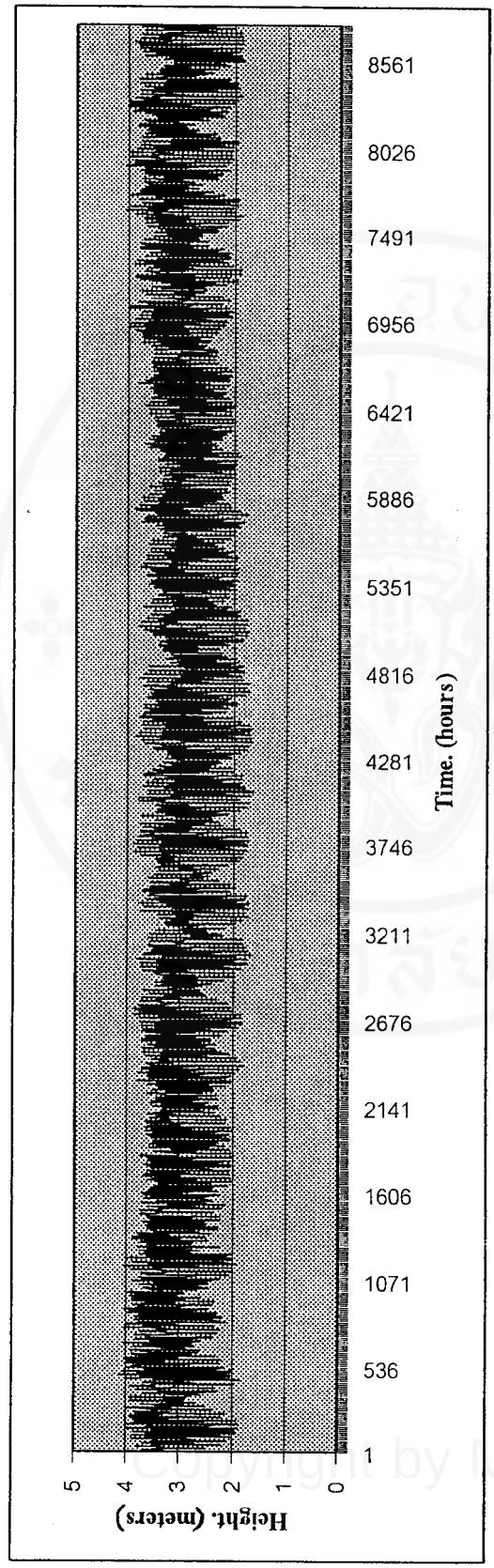

Figure 4.19 Graph of tide prediction Pak Nam Tachin station by Lagrange multipliers method

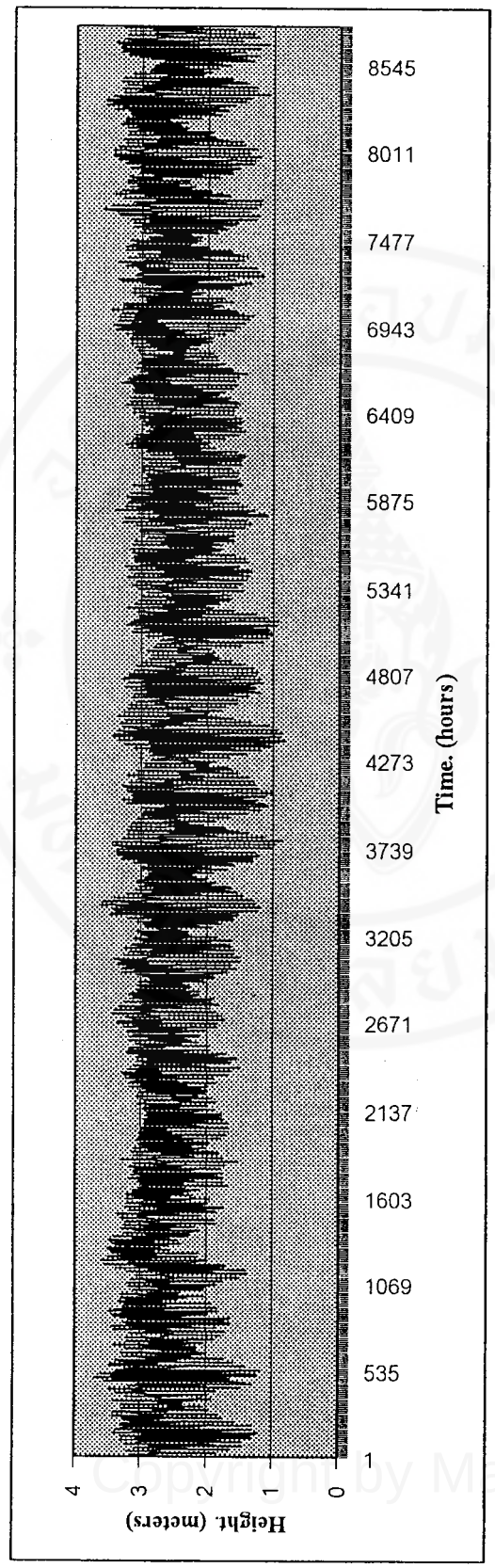

Figure 4.20 Graph of tide prediction Ko Sichang station by Lagrange multipliers method

Compare Both Results by Sum Square Error

After we have results from both methods , we use sum square error (SSE) to compare models. Table 4.6 show sum square error of each station in 1996 obtained from least square best fits and lagrange multipliers method. Table 4.7- Table 4.9 show sum square error of each station monthly obtained by the two methods.

Sum square error is defined as sum of square of the difference height of tide from data observation and prediction , i.e. ,

$$SSE = \sum_{t=1}^{n} \left(h_{obs}(t) - h_{pre}(t)\right)^2$$

where $h_{obs}(t)$ is height of tide from data observation any time.

$h_{pre}(t)$ is height of tide from prediction any time.

Figure 4.21 - Figure 4.23 show graph of sum square error to compare between least square best fits and lagrange multipliers method each station in 1996

From table 4.6 and table 4.7 , we see that values of sum square error from lagrange multipliers method are less than least square best fits in each station and from figure 4.21 – 4.23 , we have interval of sum square error of least square best fits wider than lagrange multipliers.

Table 4.6 Value of sum square error in 1996.

Station	Sum square error (SSE)	
	Least square best fits	**Lagrange multipliers method**
Hua-Hin	3057.4734	699.402
Pak Nam Tachin.	4258.2024	1201.657
Ko Sichang	4169.2424	1096.625

Table 4.7 Value of sum square error Hua-Hin station monthly in 1996.

Month	Sum square error (SSE)	
	Least square best fits	**Lagrange multipliers method**
January	265.9750	64.274
February	201.4896	44.902
March	175.0576	58.133
April	213.5499	52.060
May	241.2809	58.770
June	300.1511	70.417
July	302.9441	90.934
August	234.6921	60.514
September	170.5632	46.390
October	220.1453	56.769
November	256.7344	59.295
December	297.0829	91.446

Table 4.8 Value of sum square error Pak Nam Tachin station monthly in 1996.

Month	Sum square error (SSE)	
	Least square best fits	**Lagrange multipliers method**
January	369.1619	144.528
February	309.3562	122.907
March	317.6300	99.607
April	334.0018	105.508
May	351.6006	110.348
June	377.6101	104.652
July	387.2110	122.575
August	349.0223	117.114
September	301.2686	113.832
October	328.7088	123.522
November	321.9784	121.679
December	358.9207	116.957

Table 4.9 Value of sum square error Ko Sichang station monthly in 1996.

Month	Sum square error (SSE)	
	Least square best fits	**Lagrange multipliers method**
January	379.3664	112.002
February	255.2147	70.340
March	230.6500	68.254
April	224.7187	77.989
May	325.7471	95.410
June	423.9591	111.696
July	438.0868	135.039
August	373.4323	106.636
September	297.9616	105.111
October	349.2334	109.063
November	358.9109	96.378
December	394.1494	115.070

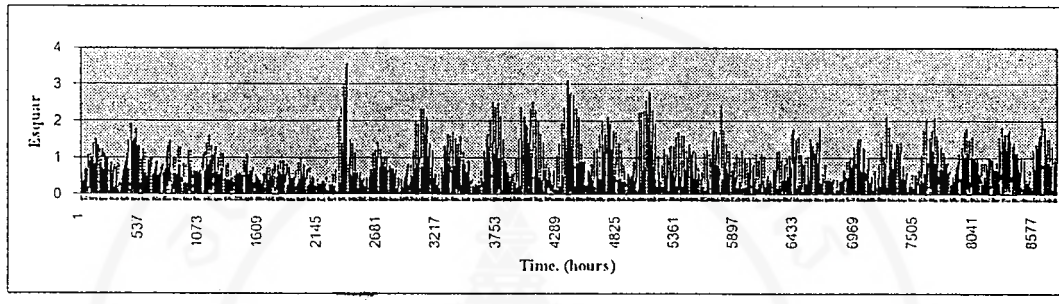

Figure 4.21(a) Graph of sum square error at Hua-Hin station by Least square best fits.

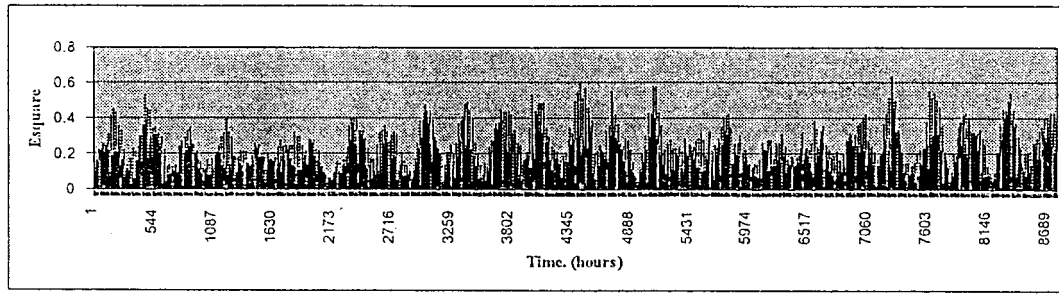

Figure 4.21(b) Graph of sum square error at Hua-Hin station by Lagrange multipliers method.

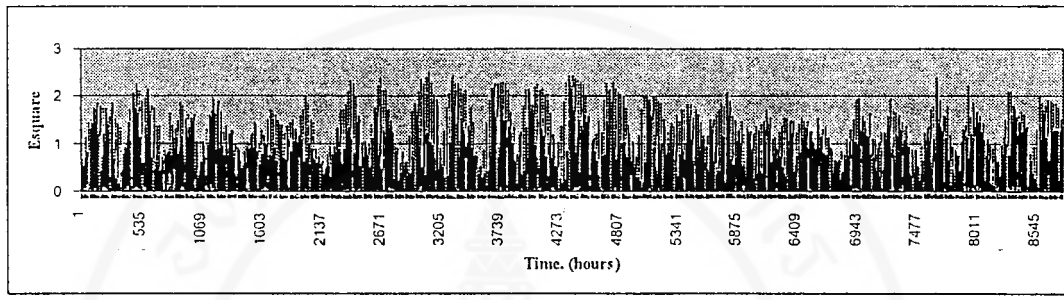

Figure 4.22(a) Graph of sum square error at Pak Nam Tachin station by Least square best fits.

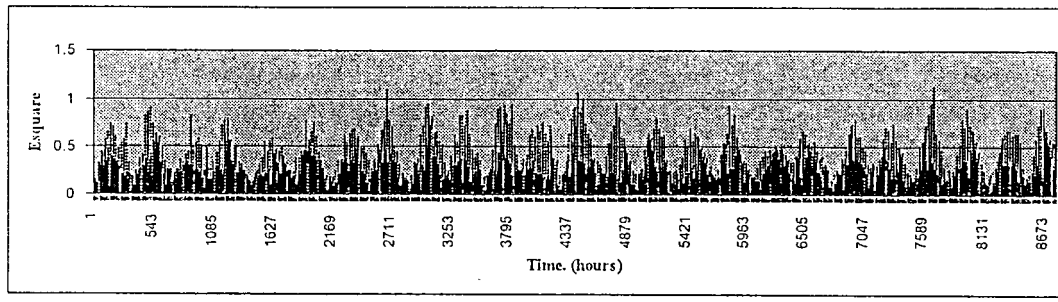

Figure 4.22(b) Graph of sum square error at Pak Nam Tachin station by Lagrange multipliers method.

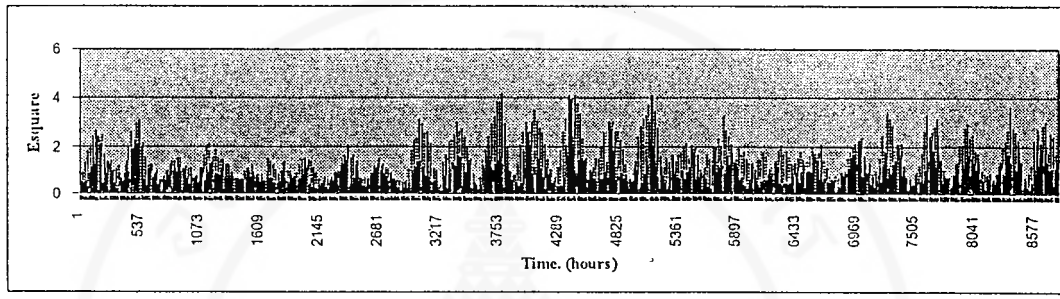

Figure 4.23(a) Graph of sum square error at Ko Sichang station by Least square best fits.

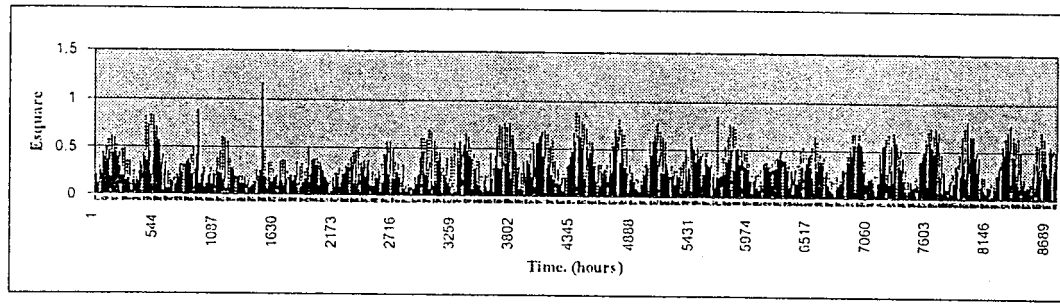

Figure 4.23(b) Graph of sum square error at Ko Sichang station by Lagrange multipliers method.

CHAPTER V

CONCLUSIONS

Over recent years there has been are increased interest in the study tidal analysis and prediction. Different method have been used to design to predict of tidal height. Data assimilation is a techniques which be combining a physical model with observational data. The physical theory for constraint equations which come from basic hydrodynamics consist of three categories :

1. Kinematical Equations
2. The Equation of Continuity
3. The Bernuolli Equation.

We have described the basic hydrodynamics in Chapter II and have described the method of calculation process, Data Assimilation techniques and Least Square Best Fits, in Chapter III. The results of model and value of sum square error from both methods including comparison of two models are given in Chapter IV.

Tidal have three types ; *diurnal tide* having a high (or a low) water in a period of a lunar day , *semidiurnal tide* having two high (or two low) waters in a period of a lunar day with almost equal height and mixed tide having two high (or two low) waters in a period of a lunar day with clearly unequal heights. In chapter IV , we see characteristics of mixed tide each station from graphs which show that all station have familiar tidal characteristics since of locations of each station aren't different regions.

In this thesis, we have studied tidal analysis and prediction in particular to the irrotational motion of an incompressible water and from Chapter II , when the pressure change are small, the density ρ is a constant and the velocity potential ϕ in an compressible liquid must satisfy Laplace's equation which the velocity potential ϕ depends on time, as well as on position.

We use physical constraint does not cover all the constraints of real tidal analysis because there are many factors that can affect behavior of tide prediction which have not been included here , some examples are the motion of moon , wind stress force , etc. So this study is only some part of the study of tidal analysis.

In this thesis, we have used VISUAL BASIC for running program and show graph by Microsoft Excel.

REFERENCES

1. Ray R.D. , Steinberg D.J , Chao B.F. , Cartwright D.E. Science 1994;264:830
2. Mccarthy D.D. IERS Standards (IERS Technical Note No. 13. Observatoire de Paris , Paris 1992; chap 7-10.
3. Hendrick R.H. ,Spiesberger J.L. , Bushong P.J. Acoust. Soc. Am. 1993;790.
4. Wunsch C. and Gaposchkin E.M. Rev. Geophys. Space Phys. 1980;725(18)
5. Fuet al. L.L , Geophys J. Res 1994;23469(99).
6. Schrama E.J.O. and Ray R.D. ibid , P.24799.
7. Ma X.C. , Shum C.K. , Eances R.J. , Tapley B.D. ibid. , P.24809
8. Egbert G.D. , Bennett A.F. , Foreman M.G. G. ibid 1994;24821(99).
9. These solutions are available at an anonymous ftp site (oce.orst.edu, /pub/tides).
10. Molines J.M. et al., in preparation.
11. Cartwright D.E. and Ray R.D. Geophys. Res. Lett. 1990;619(17).
12. Kanlaya Narue-Domkul. ON FORECASTING BANGKOK'S FLOOD [The degree of master of science ; Applied Mathematics]. Bangkok: Faculty of Graduate Studies Mahidol University;1986.
13. Hydrographic Department Royal Thai Navy. Tide tables Thai waters , Maenam Chaophraya - Gulf of Thailand and Andaman sea. Bangkok ; 1997.
14. David T. Pugh. Tides, Surges and mean sea-level. London: Jonh Wiley & Sons;1987.
15. Challis LJ. Data assimilation in ocean models. Rep.Prog.Phys.1996May; (59):1209-1266.

16. Williamson E., Crowell H. , Trotter F. Calculus of vector functions. 2nd ed. New Jersey: Prentice-Hall;1968.

17. อัปสรสุดา ศิริพงศ์ , สุทธิชัย เตมียวณิชย์. การคำนวณน้ำขึ้นน้ำลงเพื่อใช้เป็นระนาบเกณฑ์. ภาควิชาวิทยาศาสตร์ทางทะเล คณะวิทยาศาสตร์ จุฬาลงกรณ์มหาวิทยาลัย; 2525.

APPENDIX

DEFINITIONS OF SOME TIDAL TERMS

A lunar day : The interval time between two successive crossing of the meridian by the moon (mean value 24 hours 50.5 minutes).

Declination : The angular distance of an astronomical body north or south of the celestial equator, taken as positive when north and negative when south of the equator. The sun moves through a declinational cycle once a year and the moon moves through a cycle in 27.21 mean solar days. The solar declination varies between 23.5°N and 23.5°S. The cycles of the lunar declination vary in amplitude over an 18.6 year period from 28.5° to 18.5°.

Double day tide : A period of a lunar day, having two high and two low waters. This type of tides is called "Semidiurnal tide".

Duration of fall : The time interval between high water and low water.

Duration of rise : The time interval between low water and high water.

Greenwich mean time : time expressed with respect to the Greenwich Meridian(0°), often used as a standard for comparisons of global geophysical phenomena.

High water : the maximum water level reached in a tidal cycle.

Higher high water and Lower high water : on a day having two high waters, they are unequal in height, the higher being designated "the higher high water" and the lower "the lower high water".

High water interval : The time between the moon crossing a meridian (upper or lower) and the following high water. Its mean value also used for finding daily high water.

High water neap : The high water of quadrature, when the range is minimum.

High water spring : The high water of Full Moon or New Moon, when the range is maximum.

Low water : The minimum water level reached in a tidal cycle.

Lower low water and Higher low water : In a day having two low waters, they are unequal in height, the lower being designated " the lower low water" and the higher "the higher low water".

Low water interval : The time between the moon crossing a metridian (upper or lower) and the following low water.

Low water neap : The low water of quadrature.

Low water spring : The low water of Full Moon or New Moon.

Lowest low water : The lowest level of low water spring within a tidal cycle of 18.6 years.

Mean sea level : The average sea level calculated from a long series of observations obtained at equal interval of time.

Mean tide level of Half tide level : The half of height between mean high water and mean low water. This half tide level is approximately equal to mean sea level.

Mixed day tide : A period of a lunar day, having an abnormal high and low waters. This type of tides is called "Mixed tide".

Neap Range : The range of tide at neap (quadrature).

Neap rise : The heights of high water at neap above chart datum.

Range of tide : The difference in heights between consecutive high and low waters.

Single day tide : A period of a lunar day, having a high and a low water. This type of tides is called "Diurnal tide".

Spring range : The range of tide at spring.

Spring rise : The heights of high water at spring above chart datum.

Tidal datum and chart datum : Any plane of elevation level which represents the heights or the depth of tide is designated as "The tidal datum'. The tidal datum is called "Chart datum" upon using in hydrographic survey.

Tide Gauge Bench-mark : a stable bench-mark near gauge, to which tide gauge datum is referred. It is connected to local auxiliary bench-marks to check local stability and to guard against accidental damage. Tide gauge datum is a horizontal plane defined at a fixed arbitrary level below a tide gauge bench-mark.

BIOGRAPHY

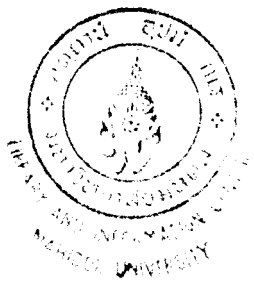

NAME Miss. Surattana Srijukkrawalwut

DATE OF BIRTH 1 Feb 1974

PLACE OF BIRTH Bangkok, Thailand

INSTITUTIONS ATTENDED

King Mongkut's Institute of Technology North Bangkok, 1991-1994.

Bachelor of Science (Applied Mathematics)

Mahidol University, 1995-2000.

Master of Science (Applied Mathematics)